EVALUATING THE DYNAMIC RESPONSE OF RETAINING WALL UNDER COMBINED RAINFALL AND SEISMIC EFFECTS

A PROJECT REPORT

submitted in partial fulfillment of the requirements for the award of the Degree of

MASTER OF TECHNOLOGY

IN

CIVIL ENGINEERING

With specialization in

STRUCTURAL ENGINEERING

Under the supervision of

Dr. Tanmay Gupta Assistant

Professor (SG)

by

Vivek Kashyap

(225024001)

To

JAYPEE UNIVERSITY OF INFORMATION TECHNOLOGY
WAKNAGHAT, SOLAN – 173234
HIMACHAL PRADESH, INDIA
May 2024

STUDENTS' DECLARATION

We hereby declare that the work presented in the project report entitled **"Evaluating the dynamic response of retaining wall under combined rainfall and seismic effect"** submitted in partial fulfillment of the requirements for the degree of Master of Technology in Civil Engineering with specialization in Structural Engineering at **Jaypee University of Information Technology, Waknaghat** is an authentic record of our work carried out under the supervision of **Dr. Tanmay Gupta.** This work has not been submitted elsewhere for the reward of any other degree/diploma. We are fully responsible for the contents of this project report.

Vivek Kashyap
225024001
Department of Civil Engineering
Jaypee University of Information Technology,
Waknaghat, India
May 2024

CERTIFICATE

This is to certify that the work which is being presented in the project report titled **"Evaluating the dynamic response of retaining wall under combined rainfall and seismic effect"** submitted in partial fulfillment of the requirements for the degree of Master of Technology in Civil Engineering with specialization in Structural Engineering at **Jaypee University of Information Technology,Waknaghat** is an authentic record of work carried out by **Vivek Kashyap (225024001)** under the supervision of **Dr. Tanmay Gupta, Assistant Professor (SG),** Department of Civil Engineering, Jaypee University of Information Technology, Waknaghat.

The above statement made is correct to the best of our knowledge.

Date: May 2024

Dr. Tanmay Gupta
Assistant Professor
Civil Engineer Department
JUIT, Waknaghat

Dr. Ashish Kumar
Professor and HOD
Civil Engineer Department
JUIT, Waknaghat

ACKNOWLEDGEMENT

This project report gives a detailed description of the study work done on the project topic **"Evaluating the dynamic response of retaining wall under combined rainfall and seismic effect"** for the partial fulfillment of the requirements for the degree of Master of Technology in Civil Engineering with specialization in Structural Engineering, under the supervision of Dr. Tanmay Gupta.

We gratefully acknowledge the Management and Administration of Jaypee University of Information Technology, Waknaghat for providing us the opportunity and hence the environment to initiate and complete our project now.

We are very grateful to our Faculty Supervisor Dr. Tanmay Gupta for his help and able guidance regarding the project. We are also very grateful to the support and assistance provided by the team of talented and dedicated technical staff comprisingMr. Jaswinder Singh of department of Civil engineering.

VIVEK KASHYAP (225024001)

TABLE OF CONTENTS

LIST OF TABLES

LIST OF FIGURES

LIST OF ABBREVIATIONS

Abbreviations	Full form
LVDT	Linear Variable Differential Transformer
FRP	Fiber Reinforced Polymer
URM	Unreinforced Masonry
RSRW	Reinforced Soil Retaining Wall
ELEP	Effective Lateral Earth Pressure
SN	Soil Nail
MSE	Mechanically Stabilized Earth
MC	Mohr Coulomb
HS	Hardening Soil
FE	Finite Element
PGA	Peak Ground Acceleration

ABSTRACT

This study presents the results of a set of shaking table tests and computational simulations conducted on a reduced-scale prototype of a retaining wall subjected to different seismic conditions. These scenarios include sine wave excitations and historical earthquake records from the Bhuj (India, 2001) and Chile (2010) earthquakes. The physical tests were conducted with different water content levels in the backfill soil: 0%, 5%, 10%, and 15% by weight. The main aim was to analyze the dynamic behavior, stability, and deformation characteristics of the retaining wall under different seismic loads and moisture conditions.

To complement the experimental findings, numerical modeling using ABAQUS was performed. The finite element analysis replicated the physical tests, providing a detailed understanding of stress distribution, failure mechanisms, and the impact of water content on dynamic response of the retaining wall.

The experimental results revealed that water content significantly affects the seismic performance of the retaining wall. Higher water content in the backfill soil resulted in greater lateral displacements and an increased likelihood of failure under both sine wave and earthquake excitations. The findings can help in designing more resilient retaining structures in earthquake-prone areas.

Keywords: Retaining wall, shaking table test, sine wave excitation, Bhuj earthquake, Chile earthquake, water content, ABAQUS, dynamic behavior, seismic performance.

CHAPTER 1

INTRODUCTION

1.1 General

Himachal Pradesh, renowned for its scenic beauty and challenging topography, has witnessed a series of devastating events like heavy rainfall during 2023 monsoon. Most of the events resulted in failure of retaining walls. Structure failures, improper drainage system, construction defect, material failure as well as natural disaster came as the real culprit for the losses incurred. The key objective of this study aims at identifying the causes and consequences of retaining wall failures, explores design improvement strategies to mitigate future disasters.

This research endeavors to confront these challenges by investigating seismic performance of retaining walls through a combination of experimental and numerical approaches. Shaking table tests were conducted on a reduced-scale model of a retaining wall, subjecting it to diverse seismic excitations. These excitations included sine wave inputs and historical earthquake records from the Bhuj (India, 2001) and Chile (2010) earthquakes, providing a thorough understanding of the wall's behavior under diverse seismic conditions. Additionally, the study explores the impact of water content in the backfill soil on the retaining wall's dynamic response. Water content levels of 0%, 5%, 10%, and 15% were tested to simulate different moisture conditions that could occur in real-world scenarios like those in Himachal Pradesh. This aspect is crucial as higher moisture levels can significantly alter soil properties and, in turn, the stability of retaining structures. Complementing the experimental work, advanced numerical simulations were carried out using ABAQUS. These simulations aimed to replicate the physical tests, offering a detailed analysis of stress distribution, failure mechanisms, and overall dynamic behavior under seismic loading. By bridging the gap between experimental data and numerical predictions, this research offers valuable insights into the factors influencing the seismic performance of retaining wall.

A retaining wall is a structure designed to withstand lateral pressure of soil or to hold back soil particles. Various factors such as liquid pressure, earth filling, sand, and other granular matter behind the retaining wall structure contribute to the lateral pressure it experiences. Retaining wall give infrastructure and landscapes structural support while preserving the stability of slopes and

reducing soil erosion. Static loads, dynamic forces, seismic occurrences, and other environmental factors are all things that retaining walls are made to withstand while maintaining the long-term stability and safety of the surrounding area.

1.2 Types of Retaining Wall

Different types of retaining wall categorized on the basis of their uses and material are as follow-

i. Gravity retaining wall
ii. Counterfort retaining wall
iii. Cantilever retaining wall
iv. Gabion retaining wall
v. Anchored retaining wall
vi. Crib retaining wall
vii. Sheet pile retaining wall
viii. Mechanical stabilized earth retaining wall

1.2.1 Gravity Retaining Wall

In a Gravity Retaining Wall, the wall's weight resists lateral earth pressure. Gravity Retaining walls require a large gravity load to endure the horizontal soil pressure because the wall's own weight is its only means of resistance. When building a gravity retaining wall, the forces of sliding, overturning, and bearing have to be considered because these are the main causes of the wall's collapse. A range of building materials, including stone, concrete, and masonry components, can be used to construct it. In recent years, gabion and crib retaining walls have gained popularity as typical gravity retaining walls.

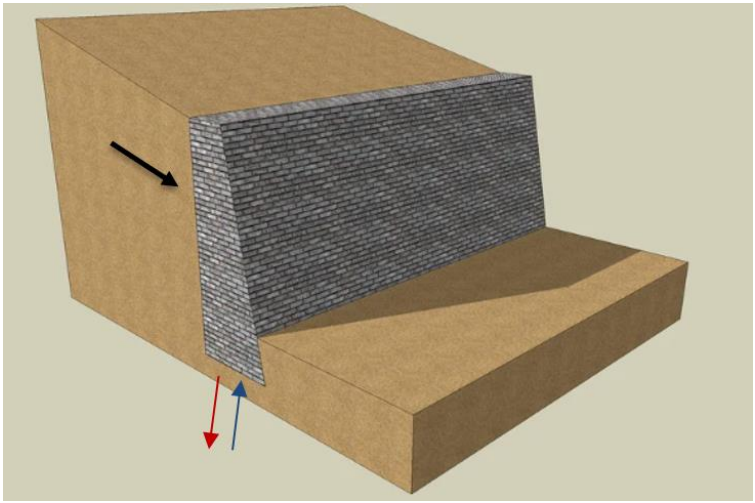

Fig.1.1 Gravity Retaining Wall

1.2.2 Cantilever Retaining Wall

Cantilever retaining walls operate on the principle of leverage and are typically constructed using reinforced concrete. They rely on the weight of the backfill soil to offer substantial resistance against sliding and overturning, with a comparatively thinner stem. The cantilever retaining wall's two primary parts are the base slab and the stem. A portion of the base slab is beneath the backfill. Cantilever retaining wall is one of the most popular designs for earth-retaining walls. This wall sits on the slab foundation and is attached to it. Precast concrete, prestressed concrete, or reinforced concrete can be used to build these walls. For a maximum of ten metres, this kind of retaining wall is employed. Interestingly, the cantilever retaining walls have vertical toe and heel. This type of retaining wall utilises less concrete than a gravity retaining wall. There are three possible reasons for a cantilever retaining wall to fail: soil bearing pressure, uplift pressure, and sliding.

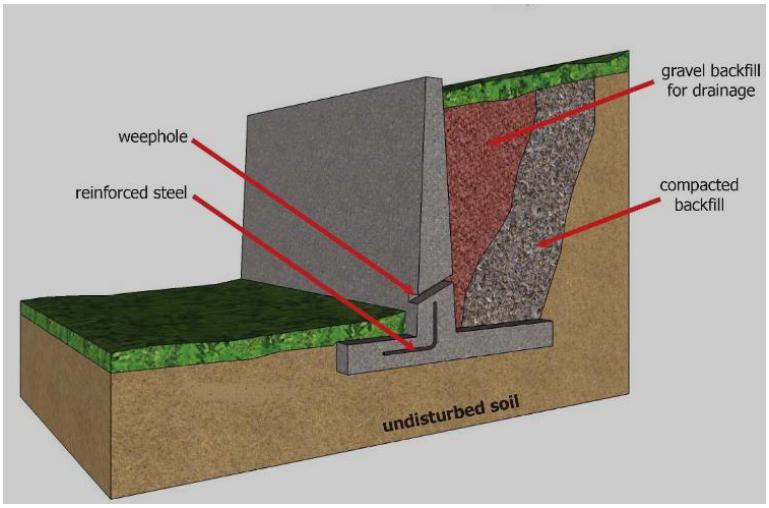

Fig.1.2 Cantilever Retaining Wall

1.2.3 Counterfort Retaining Wall

These walls are made up of counterforts, which are slender vertical webs of concrete spaced regularly along the wall's back. For heights over eight metres, they are utilizedl. This counterfort acts monolithically with both the slab and the foundation, uniting them. Counterforts are spaced more than half the height apart.

Fig.1.3 (a) Counterfort Retaining Wall

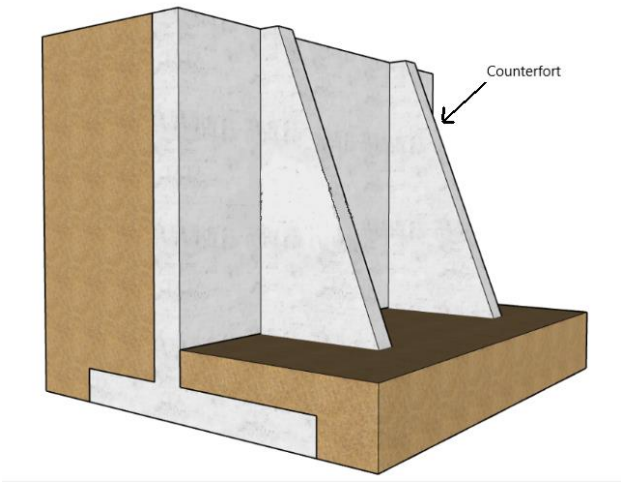

Fig.1.3 (b) Counterfort Retaining Wall

1.2.4 Gabion Retaining Wall

These walls are made of stone-filled gabions that are firmly attached to the wire. Gabion Stainless steel wires or galvanised steel wires are commonly used to build retaining walls. Typically, these walls are intended to stop roadways, riverbanks, and other sloping areas from eroding.

Fig.1.4 Gabion Retaining Wall

1.2.5 Anchored Retaining Wall

A retaining wall that is reinforced by cables or anchors buried in the ground behind it is known as an anchored retaining wall. To provide the wall more stability and support, the anchors are tensioned. Tall or highly loaded walls are frequently constructed with anchored retaining walls. The anchor in this wall resist soil pressure. The anchors produce opposing forces to avoid instances that could result in the wall toppling and slipping. Interestingly, these anchors can withstand heavy loads and are loaded axially.

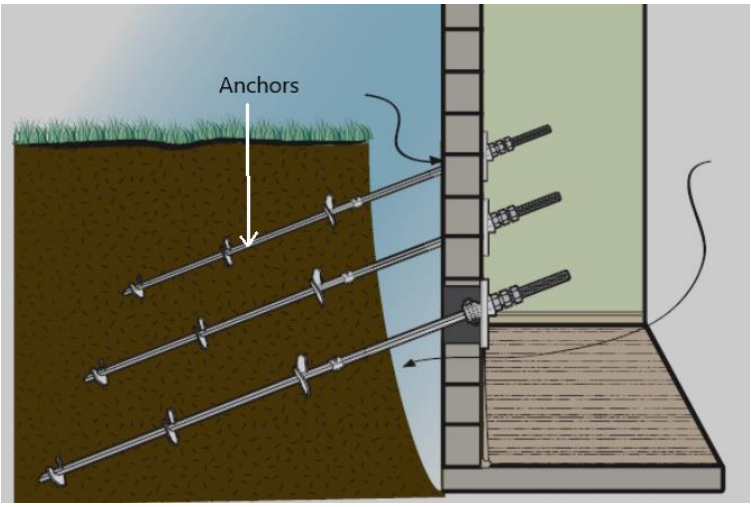

Fig.1.5 Anchored Retaining Wall

1.2.6 Crib Retaining Wall

One type of gravity wall is the crib retaining wall. They are built from individual, interconnected boxes composed of precast concrete else wood. The boxes are filled with crushed stone or other coarse granular materials to create a structure with effective drainage. Precast reinforced walls and timber retaining walls are the two fundamental types of crib retaining walls are. It works well supporting planting areas, but supporting slopes or buildings with it is not advised.

Fig.1.6 Crib Retaining Wall

1.2.7 Sheet Pile Retaining Wall

They consist of connected piles that have been pushed into the foundational soil. Sheet piles can be made of precast concrete, steel, or wood. The soil pressure at the retaining wall's base stabilizes the Sheet pile retaining wall.

Fig.1.7 Sheet Pile Retaining Wall

1.2.8 Mechanically stabilized earth retaining wall

One of the most commonly utilized and economical types of retaining wall is the mechanically stabilized earth (MSE) retaining wall. MSE walls are constructed with reinforcements, such as plastic meshes or metallic strips, and are supported by specific fill materials, typically granular in nature. Examples of MSE retaining wall types include panel walls, temporary earth retaining walls and concrete block walls.

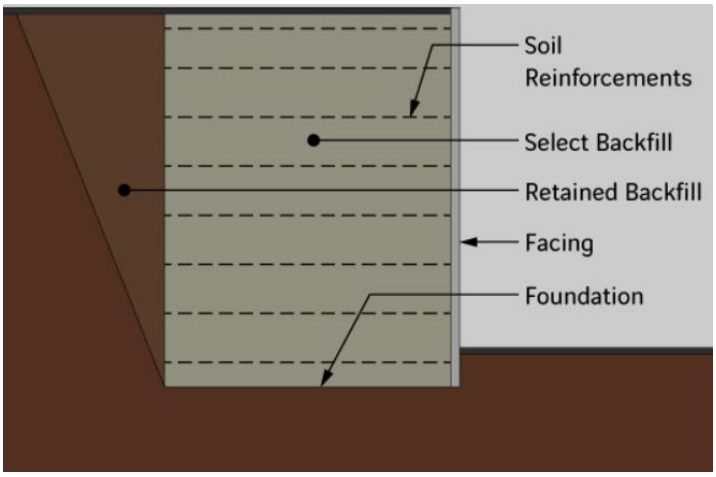

Fig.1.8 Mechanical Stabilized Earth Retaining Wall

1.3 Applications of Retaining Wall

Retaining walls are used in many civil engineering and landscaping projects as a means of solving challenges including soil stability, ground elevation variations, and erosion management. The following are a few typical uses for retaining walls:

i. In order to stabilize slopes and hillsides and stop soil erosion and landslides, retaining walls are widely used. They offer structural support to preserve the terrain's integrity.

ii. Retaining walls are important in construction of highway and roads to develop level surface generally for hilly and mountain regions. They prevent soil mass to enter the roads and helps to maintain alignment of road.

iii. Retaining wall can also serve the purpose of wing walls and abutments in construction of bridges. They provide support to bridge and stabilizes the soil.

iv. In stormwater management systems, retaining walls are used to direct and regulate flow of water. By regulating the fluctuations in elevation within a landscape, they aid in the prevention of soil erosion and promote appropriate drainage.

v. In mining and quarrying activities, retaining walls are used to regulate the integrity of excavated slopes. They assure safe working conditions and stop falling rocks or soil from collapsing.

vi. Retaining walls are used in coastal locations to prevent shorelines from erosion carried on by tidal and wave action. One kind of retaining wall that helps stop coastal erosion and safeguards waterfront properties is a seawall.

1.4 Scope of Thesis

This thesis presents an extensive investigation into the retaining walls seismic behavior using both experimental and numerical methods. It involves various shaking table tests on a scaled-down retaining wall model subjected to various seismic excitations, including sine wave inputs and actual earthquake records from the Bhuj (India, 2001) and Chile (2010) earthquakes. Additionally, the study explores the impact of different water content levels in the backfill soil specifically 0%, 5%, 10%, and 15% to understand how moisture affects the wall's dynamic response and stability. To complement the physical experiments, sophisticated numerical simulations using ABAQUS are conducted, providing a thorough analysis of stress distribution, failure mechanisms, and the overall behavior of the retaining wall under seismic loading. The thesis seeks to bridge the gap between experimental findings and numerical predictions, offering detailed insights into the factors influencing the seismic performance of retaining walls. This research has significant implications for the design and analysis of retaining structures, particularly in earthquake-prone areas, and contributes to the development of safer and more resilient infrastructure.

1.5 Organization of Thesis

This study demonstrates the effective utilization of waste materials with minimal environmental impact. The thesis structure is as follows:

Chapter 2 examines relevant research papers, highlighting distinctions from previous studies.

Chapter 3 outlines the methodology, encompassing tests, and experimental study.

Chapter 4 discuss modelling and analysis of retaining wall in Abaqus.

Chapter 5 presents test results and analyses of retaining wall under different seismic excitation.

Chapter 6 summarizes the conclusions drawn from all tests.

CHAPTER 2

LITERTAURE REVIEW

2.1 General

This chapter covers different studies done on dynamic analysis of retaining walls and retrofitting strategies on shaking table. Different types of wall like geogrid reinforced, drystone, brick, geocell facing, polymer reinforced are tested. Also this chapter tells us about the researches done in past to understand the test setup and their results. The whole setup is equipped with strain gauges, accelerometers, force and laser displacement transducers. The test model were given different excitation and earthquakes like Kobe, Bhuj, Chile. Seismic response of different retaining walls is analyzed. The key observation like geogrids length, height of facing wall, polymer reinforced wall etc. are drawn.

2.2 REVIEWS

O. Matsuo, T. Tsutsumi, K. Yokoyama and Y.Saito (1998)

The study examines how geosynthetic reinforced soil (GRS) retaining walls perform under seismic conditions through a combination of experimental shaking table tests and numerical analyses. The study demonstrates that GRS walls exhibit superior stability and reduced deformations compared to unreinforced walls when subjected to earthquake-induced shaking. The experimental setup involved sensors to measure displacements and accelerations, revealing that geosynthetic reinforcement significantly enhances wall stability and mitigates deformation patterns during seismic events. Complementary numerical simulations validated the experimental findings and provided deeper insights into the soil geosynthetic interaction under dynamic loading. The research highlights the practical benefits of using geosynthetics for seismic reinforcement of retaining walls, offering valuable recommendations for design and construction in earthquake-prone areas.

Hoe I. Ling, Y. Mohri, D. Leshchinsky, H. Liu (2005)

The paper investigates the seismic behavior of modular-block reinforced soil (MBRS) retaining walls by conducting large-scale shaking table experiments. These tests simulated earthquake conditions to assess the walls' behavior, including displacement, acceleration, and failure modes. Constructed with modular blocks and reinforced with geosynthetic materials, the walls demonstrated significant resilience to seismic forces, maintaining stability with reduced displacements and deformations. The geosynthetic reinforcement effectively enhanced the structural integrity of the walls during dynamic loading, and specific failure mechanisms and deformation patterns were identified. Complementary numerical simulations validated the experimental results, providing broader insights into the interaction between modular blocks, soil, and geosynthetics under earthquake conditions. The study highlights the practical benefits of MBRS systems, offering design guidelines for constructing earthquake-resistant retaining walls, and concludes that properly reinforced MBRS walls exhibit robust performance under seismic loading, contributing valuable knowledge to geotechnical and earthquake engineering practices.

Hoe I. Ling, D. Leshchinsky, J. Pin Wang, Y. Mohri, and A. Rosen (2009)

The paper investigates the seismic performance of geocell retaining walls through a series of experimental studies. The research involved conducting shaking table tests to simulate earthquake conditions and evaluate the dynamic response of geocell-reinforced retaining walls. These tests aimed to measure displacements, accelerations, and identify potential failure mechanisms. The study found that geocell reinforcement significantly improved the seismic stability of retaining walls, reducing deformations and enhancing overall structural integrity under dynamic loading. Specific patterns of wall behavior and failure were observed, providing insights into the mechanisms of geocell reinforcement during seismic events. The findings suggest that geocell-reinforced walls can effectively withstand seismic forces, offering practical benefits for earthquake-resistant design in geotechnical engineering. This research contributes valuable data and design recommendations for the application of geocell technology in constructing resilient retaining walls in seismically active regions.

Q. Ma, S. Beskhyroun, L. Wotherspoon, G. Simkin & J. Ingham (2014)

The paper examines the inter storey drifts experienced by buildings throughout the Cook Strait earthquake sequence. The research involves detailed experimental evaluations to measure and analyze the inter storey drifts, which are critical indicators of building deformation and potential damage during seismic events. The study utilized data from various buildings affected by the earthquake sequence, assessing the performance and resilience of different structural designs. Findings highlighted significant variations in inter-storey drift responses, influenced by factors such as building height, construction materials, and structural systems. The research provides insights into the behavior of buildings under seismic loading, emphasizing the importance of designing structures to accommodate inter-storey drifts and enhance earthquake resilience. These findings contribute to improving building codes and design practices for better seismic performance and safety in earthquake-prone regions.

Anissa Maria Hidayati, Sri Prabandiyani RW, I Wayan Redana (2015)

The paper investigates the failure mechanisms of retaining walls under sinusoidal loading conditions. The study involves laboratory tests designed to simulate the effects of sinusoidal loads, which mimic the dynamic forces experienced during seismic events, on retaining walls. The researchers constructed model retaining walls and subjected them to controlled sinusoidal loads, meticulously measuring the resulting displacements, stresses, and failure patterns. The findings reveal that sinusoidal loading significantly impacts the stability of retaining walls, leading to various modes of failure depending on the load frequency and amplitude. Key observations include the identification of critical load conditions that precipitate wall failure and the characterization of deformation patterns that precede structural collapse. This research provides valuable insights into the dynamic behavior of retaining walls under seismic-like conditions, offering important implications for the design and construction of more resilient retaining structures in areas susceptible to dynamic loading.

M. Umair Saleem, M. Numada, M. Nasir Amin, K. Meguro (2016)

The paper explores the seismic performance of masonry buildings retrofitted with Fiber

Reinforced Polymer (FRP) through a series of shake table tests. The study aims to evaluate the effectiveness of FRP retrofitting in enhancing the seismic resilience of masonry structures. Researchers constructed masonry building models and subjected them to simulated earthquake conditions using a shake table. The tests measured various parameters, including displacements, accelerations, and failure modes, to assess the structural improvements imparted by the FRP retrofits. The results indicated that FRP retrofitting significantly enhances the seismic performance of masonry buildings, reducing displacements and preventing catastrophic failures. Specific observations included improved stiffness, strength, and energy dissipation capabilities of the retrofitted models. This research underscores the potential of FRP materials in strengthening existing masonry structures against seismic forces, providing practical insights and guidelines for the application of FRP retrofitting techniques in earthquake-prone regions.

G. Madhavi Latha G. S. Manju (2016)

The paper examines the seismic behavior of geocell retaining walls through shaking table experiments. The study aims to understand how geocell reinforcement affects the stability and behavior of retaining walls under earthquake loading conditions. A series of shaking table tests were conducted on model retaining walls reinforced with geocells, measuring parameters such as displacements, accelerations, and failure mechanisms. The results showed that geocell reinforcement significantly enhances the seismic stability of retaining walls by reducing lateral displacements and preventing catastrophic failures. The geocell-reinforced walls exhibited improved energy dissipation and greater overall resilience under dynamic loading compared to unreinforced walls. This research provides valuable insights into the effectiveness of geocell technology in effectively increasing the seismic performance of retaining structures, offering practical recommendations for designing earthquake-resistant retaining walls in geotechnical engineering applications.

Jie Ai, Jin song Gui, Ding Chen (2016)

The study explores the use of the Abaqus finite element software to analyze retaining walls earth pressure. The study aims to gain a comprehensive understanding of the distribution and magnitude of earth pressure exerted on retaining structures, which is critical for their design and stability. Using the Abaqus software, the researchers created a numerical model to simulate various conditions affecting earth pressure, such as different soil types, wall stiffness, and loading

scenarios. The analysis provided insights into how these factors influence the earth pressure distribution along the height of the retaining wall. Key findings included the identification of critical pressure zones and the impact of wall-soil interaction on overall wall performance. This research contributes to more accurate and reliable design methodologies for retaining walls by leveraging advanced simulation techniques, ultimately enhancing their safety and effectiveness in civil engineering applications.

A. Johari, A.A. Javadi and H. Naja (2016)

The paper introduces a genetic-based model aimed at predicting the maximum lateral displacement of retaining walls in granular soil. The study addresses the challenge of accurately estimating the lateral displacement of retaining walls, which is crucial for their design and stability assessment. By employing genetic algorithms, the researchers developed a predictive model capable of accounting for various factors influencing lateral displacement, such as soil properties, wall geometry, and loading conditions. The model's effectiveness was validated through comparisons with experimental data and existing analytical solutions, demonstrating its ability to accurately predict lateral displacements under different scenarios. This research contributes to improving the understanding and prediction of retaining wall behavior in granular soil, offering valuable insights for engineers involved in geotechnical and civil engineering projects.

Weiwei Li, Shuguang Wang, Weiqing Liu and Dongsheng Du (2017)

The paper investigates the effectiveness of pre-fabricated concrete walls in strengthening masonry structure against in-plane seismic forces through shaking table tests. The study aims to evaluate the performance of prefabricated concrete walls as retrofitting measures for enhancing the seismic resilience of masonry buildings. Utilizing a shaking table, the researchers subjected model masonry structures, both retrofitted with prefabricated concrete walls and non-retrofitted, to simulated seismic excitations. The tests measured parameters such as displacements, accelerations, and failure modes to assess the retrofitting effectiveness. The results demonstrated that prefabricated concrete walls significantly improved the in-plane strength and stiffness of masonry structures, reducing deformations and enhancing overall seismic performance. This research provides valuable insights into the application of prefabricated concrete walls as a retrofitting

technique for masonry buildings, offering practical implications for seismic retrofitting strategies in earthquake-prone regions.

M. Yazdandoust (2017)

The paper explores the seismic performance of steel-strip reinforced soil retaining walls using shaking table tests. The study aims to assess the effectiveness of steel-strip reinforcement in enhancing the seismic resilience of soil retaining structures. Model retaining walls were subjected to shaking table tests, with and without steel-strip reinforcement, to simulate earthquake-induced dynamic loading. The tests measured parameters such as displacements, accelerations, and failure mechanisms to evaluate the seismic performance of the walls. The results indicated that steel-strip reinforcement significantly improved the stability and deformability of the retaining walls under seismic loading, reducing displacements and mitigating failure modes. This research contributes to advancing the understanding of steel-strip reinforced-soil retaining wall systems and provides practical insights for their design and construction in earthquake-prone regions.

Shi-Yu Xu, Ertugrul Taciroglu, K.K. Pabodha M. Kannangara (2018)

The paper investigates stress distribution within the backfill material behind a retaining wall. The study aims to enhance understanding the interactions between retaining wall and its surrounding soil, which is crucial for the design and performance assessment of such structures. Using numerical modeling techniques, the researchers analyzed the stress distribution across the backfill under various loading conditions. The analysis considered factors such as soil properties, wall geometry, and loading characteristics to accurately predict stress distributions. The findings provide insights into the behavior of retaining walls with different scenarios, offering valuable information for optimizing design parameters and improving the stability and performance of retaining structures. This research contributes to advancing the field of geotechnical engineering by providing a better understanding of stress distribution mechanisms within retaining wall backfills, facilitating more efficient and resilient design practices.

Yu-liang Lin, Xue-ming Cheng, Guo-lin Yang (2018)

The paper investigates the response of a combined retaining structure to earthquake loading

through shaking table tests and numerical simulations. The study aims to understand the dynamic behavior of combined retaining structures under seismic conditions, which consist of different retaining elements such as soldier piles, soil nails, and reinforced soil. Shaking table tests were conducted to simulate earthquake-induced motions, while numerical simulations were employed to further analyze and validate the experimental results. The research provides insights into the interaction between the various components of the combined retaining structure, as well as their collective response to seismic loading. The findings contribute to improving the design and performance assessment of combined retaining structures, enhancing their resilience and stability in earthquake-prone areas.

Juan C. Reyes et.al (2019)

The paper presents the findings of shaking table tests conducted on full-scale historic adobe corner walls retrofitted with timber elements to improve their out-of-plane seismic resistance. The study aims to evaluate the effectiveness of timber retrofitting techniques in enhancing the seismic performance of traditional adobe structures. Through shaking table tests, the researchers subjected the retrofitted corner walls to simulated earthquake motions to assess their behavior and resilience. The results provide valuable insights into the effectiveness of timber retrofitting in mitigating out-of-plane failure modes and improving the seismic resistance of historic adobe structures. This research contributes to the development of retrofitting strategies for preserving and strengthening traditional masonry buildings against seismic hazards, thereby enhancing their safety and resilience.

N. Savalle, E. Vincens & S. Hans, J. Blanc-Gonnet (2020)

This paper presents the results of an experimental investigation designed to investigate seismic behavior of dry stone retaining walls. Tests using a shaking table have been performed on smaller dry joint retaining walls made of parallelepiped bricks. It is discovered that a certain retaining wall is less susceptible to higher frequencies and that a thicker wall is more resistant. The walls can withstand greater displacements before crumbling at those higher frequencies. The displacements begin at a specific threshold, which is determined by the geometry of the wall but not by frequency of base motion. Typically, low frequency inputs and/or thin walls result in toppling failures. When

walls are not as thin or when input frequencies are higher, there are local sliding failures in the walls that lead to the system's total collapse. By comparing the acceleration at failure observed during dynamic tests to the corresponding pseudo-static resistance, a careful calculation of the seismic behavior coefficient for pseudo-static analysis of this type of retaining wall has been achieved. The purpose of this unique experimental dataset is to provide a foundation for validating upcoming analytical or numerical tools in the field.

Feifan Ren, Qiangqiang Huang, Guan Wang (2020)

The paper investigates behavior of reinforced soil retaining wall under the simultaneous influence of rainfall and earthquakes. The study addresses the critical issue of considering multiple environmental factors that can affect the stability and performance of retaining walls. Through shaking table tests, the researchers simulated the combined effects of seismic shaking and rainfall infiltration on reinforced soil retaining walls to assess their response and resilience. The findings offer valuable insights into how these interacting factors impact the stability and deformation behavior of retaining walls, providing essential information for improving design methodologies and risk assessment practices in geotechnical engineering. This research contributes to enhancing our understanding of the complex interactions between natural hazards and engineered structures, ultimately leading to more robust and resilient infrastructure development strategies.

Rohit Tiwari, Nelson Lam (2021)

The paper focuses on modeling seismic actions in earth retaining walls and comparing the results with experimental data obtained from shaker table tests. The study aims to improve the understanding and prediction of the behavior of earth retaining walls under seismic loading conditions. Using numerical modeling techniques, the researchers simulate seismic actions on retaining walls and compare the results with experimental data obtained from shaking table test. By evaluating the agreement between the numerical simulations and experimental observations, the study validates the accuracy of the modeling approach in predicting the seismic response of earth retaining walls. The findings provide valuable key insights into the seismic behavior of retaining walls and add-on to the development of reliable design methodology for such structures in earthquake-prone areas. This research enhances our ability to assess the seismic performance of earth retaining walls and supports efforts to design resilient infrastructure capable of withstanding

seismic events.

Shuzhi Ma, Xiaolang Liu, Hongbiao Jia (2022)

The paper investigates the impact of the wall back inclination angle on distribution of inertial loading along gravity-retaining walls through experimental shaking table test. The study aims to understand how varying inclination angles of the wall-back affect the distribution of inertial forces exerted on the retaining wall during seismic events. Through shaking table experiments, the researchers systematically vary the inclination angle of the wall back and measure the resulting distribution of inertial loading along the wall. The findings provide insights into how changes in the wall back inclination angle influence the magnitude and distribution of inertial forces, which are crucial factors in the design and performance assessment of gravity-retaining walls under seismic loading conditions. This research contributes to advancing understanding of the behavior of gravity-retaining walls and informs more effective design strategies for enhancing their seismic resilience.

V. Sundaravel, G. R. Dodagoudar (2024)

The paper focuses on the finite element analysis (FEA) of reinforced earth retaining structures. The study aims to investigate various material models used in FEA and assess the performance of reinforced retaining earth structures under different loading. Through numerical simulations using finite element analysis, the researchers explore the behavior of reinforced earth structures with different reinforcement types, soil properties, and loading scenarios. The study evaluates the accuracy and applicability of different material models in predicting the response of reinforced earth retaining structures and assesses their performance in terms of stability, deformation, and bearing capacity. The findings provide valuable key insights into the behavior of reinforced earth structures and offer guidance for selecting appropriate material models for accurate performance assessment in geotechnical engineering practice. This research contributes to advancing the understanding and design methodologies for reinforced earth retaining structures, supporting more efficient and reliable infrastructure development in civil engineering projects.

2.3 RESEARCH GAPS

- Retaining wall design are generally based on static behavior considering only factor of safety therefore dynamic analysis is needed.
- There is no large scale testing done for retaining walls.

2.4 OBJECTIVES

Based on a review of the literature, the following objectives have been established -

1. To understand causes of retaining wall failure and model retaining wall in laboratory setup.
2. To study the dynamic effect of retaining wall under various dynamic excitation and rainfall condition via shake table.
3. To compare and validate the results of shake table by simulating seismic excitation in Abaqus.

CHAPTER 3
METHODOLOGY AND EXPERIMENTAL STUDY

3.1 METHODOLOGY

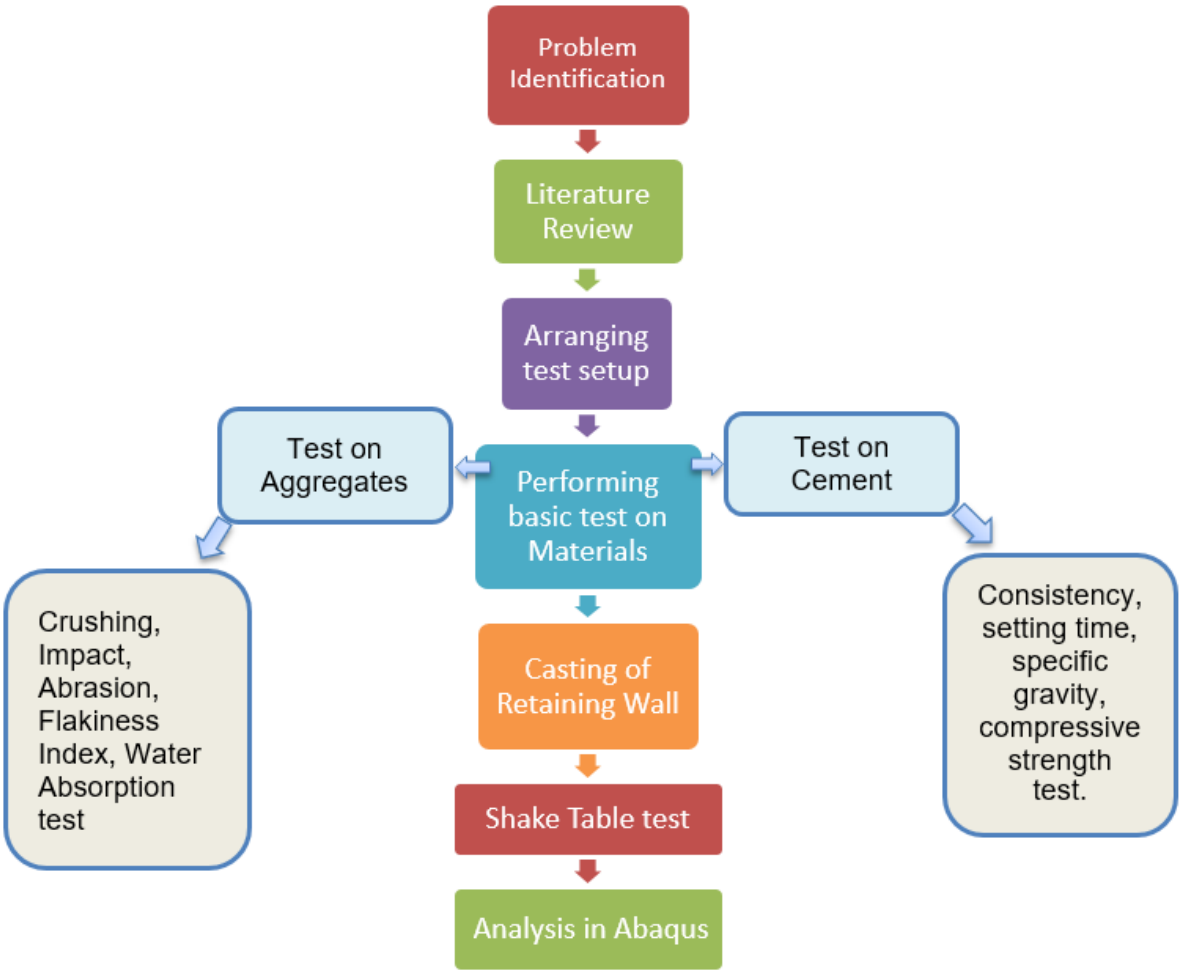

Fig. 3.1 Flow chart of methodology

3.2 EXPERIMENTAL STUDY

MATERIAL PROPERTIES

3.2.1 AGGREGATES

Aggregate plays an important role in the construction of pavement. Aggregates main motive is to absorb and transfer the live load from road to ground. Hence, it is important to know different qualities and features of the aggregate. They should resist abrasive action of load coming from wheels. Different types and grades of aggregates are usedto make bituminous pavement. To know different properties of the aggregates, following tests are performed in the lab

i. Crushing test
ii. Los angeles abrasion test
iii. Impact test
iv. Shape test
v. Soundness test
vi. Water absorption test
vii. Specific gravity test

Table 3.1 Basic Aggregate test values

S.No.	Experiment	Value
1.	Aggregate Impact Value	16.93%
2.	Aggregate Crushing Value	23.84%
3.	Specific Gravity (aggregates)	1.83
4.	Water Absorption (aggregates)	1.14%
5.	Los Angeles Abrasion Test	32.53%

3.2.2 CEMENT

Cement is a finely ground mineral powder, typically grey in appearance. In construction, cement acts as a binder that sets, hardens, and adheres to other materials, effectively binding them together. It is mainly used to bond materials such as sand and is seldom used on its own. Masonry mortar is created by mixing cement with fine aggregate, while concrete is produced by combining cement with sand and gravel. Concrete is the most widely used substance on Earth, second only to water in terms of consumption. To find various cement properties, following tests are performed -

i. Consistency test
ii. Setting time
iii. Specific Gravity test
iv. Compressive Strength test

Table 3.2 Basic Cement test values

S.No.	Experiment	Value
1.	Fineness of Cement	7.85%
2.	Normal consistency	33.1%
3.	Initial setting time	37 min
4.	Final setting time	463 min
5.	Specific gravity	3.12
6.	Soundness Test	4.27 mm

3.2.3 COMPRESSIVE STRENGTH OF M15 CONCRETE

Table 3.3 Compressive strength of concrete

No. of Days	Compressive strength of concrete (MPa)		
	Sample 1	Sample 2	Sample 3
3	6.56	6.89	6.32
7	9.49	9.84	9.59
28	14.23	14.58	15.09

3.3 STRAIN GAUGES

Strain gauges serve as instruments employed for gauging the strain exerted on an object. Strain denotes the degree of deformation experienced by an object when subjected to an external force, often quantified as a proportion or percentage of its original dimensions. Typically comprising a slender wire or foil affixed to a support material, strain gauges deform along with the object to which they are attached, altering their electrical resistance. This change in resistance is then measured to ascertain the extent of strain endured by the object. Widely utilized across engineering and materials analysis, strain gauges are pivotal for evaluating stress and strain in various structures, including bridges, edifices, aircraft, and industrial equipment. Moreover, they find application in the development and assessment of materials and components within domains such as aerospace, automotive engineering, civil engineering, and biomechanics. Through furnishing invaluable data, they contribute significantly to assuring the structural robustness, efficiency, and safety of diverse systems and constituents. The strain gauge used in our experiment was 5mm with 350 ohm resistance.

Fig.3.2 (a) Pasting strain gauges

Fig.3.2 (b) Strain gauge

Fig. 3.2 (c) Calibrating strain gauges

Fig.3.2 (d) Strain gauge with loads

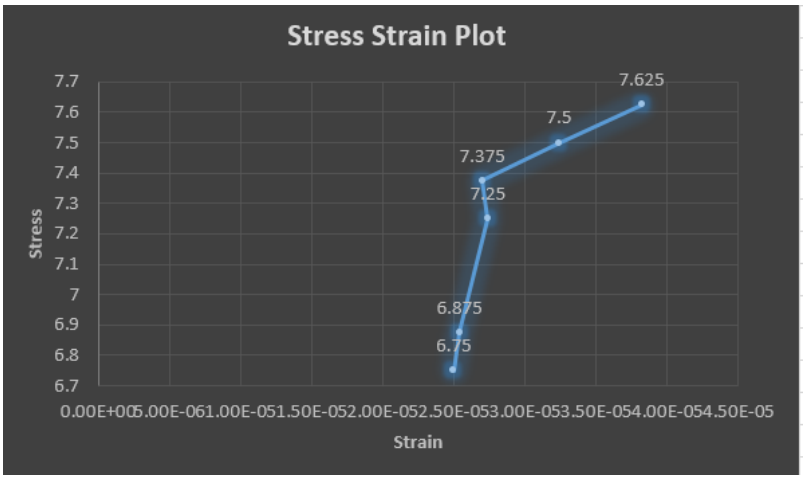

Strain	Stress (MPa)	E (Mpa)
2.50E-05	6.75	2.70E+05
2.54E-05	6.875	2.71E+05
2.74E-05	7.25	2.65E+05
2.70E-05	7.375	2.73E+05
3.24E-05	7.5	2.31E+05
3.82E-05	7.625	2.00E+05
	Avg =	2.52E+05

Fig.3.3 Strain gauge calibration

3.4 DATA LOGGER

A strain gauge data logger is a specialized device crafted to gather, retain, and occasionally transmit data derived from strain gauges. Typically, it comprises a central unit furnished with ports or channels for linking multiple strain gauges, alongside internal memory or storage capability for preserving the acquired data. These loggers find utility across diverse sectors like civil engineering, aerospace, automotive, and materials testing, especially in scenarios necessitating continual monitoring of structural stability or functionality over prolonged durations. The strain gauge data logger documents alterations in electrical resistance stemming from the strain gauges as they undergo deformation in reaction to applied forces or loads. Subsequently, this data can be scrutinized to evaluate aspects such as stress distribution, fatigue, and overall structural condition.

Fig.3.4 Data Logger to measure strain values

3.5 PREPARATION OF CONTAINER

The model container depicted in Figure is created specifically to conduct model testing on embankments. To produce or imitate a model ground, a 12-mm-thick acrylic sheet container with a top opening was utilized. Acrylic sheet is used for the container to clearly see during shaking from any angle. Because of structural considerations, the container has to be 12 mm thick in order to withstand cantilever action and lateral bending. Acrylic sheet was measured and cut into desired measurement with the help of cutter from work lab with all required safety precaution. Though the container is made by welders. The container's external measurements were 720 mm in depth, 1200 mm in length, and 1000 mm in width. The length and width of the chosen dimensions were sufficient to replicate one-dimensional model studies of geotechnical infrastructure, such as retaining walls, sloped terrain, and embankments.

Fig.3.5 (a) Acrylic sheets of required length

Fig.3.5 (b) Welding of Container

3.6 PREPARATION OF FORMWORK

With scaling factor of 1:100 retaining wall of height 6m, top width .60m, bottom width 2.80m, and length .96m is decided according to our container. The slope of 1:5 is given to the retaining wall. To attain the accurate slope two pieces of fly ash blocks are taken and proper measurement and marking is done. Cutting of the blocks is done with the help of saw as shown in the figure. The rest of the formwork like ply board are taken from the workshop lab and placed with the support of concrete blocks.

Fig.3.6 (a) Dimensioning of retaining wall

Fig.3.6 (b) Dimensioning of slope

Fig.3.6 (c) Formwork Arrangement

3.7 RETAINING WALL CASTING

Grades of concrete are defined by the strength and composition of the concrete, and the minimum strength the concrete should have following 28 days of initial construction. The grade of concrete is understood in measurements of MPa, where M stands for mix and the MPa denotes the overall strength. There are many categories of nominal mix of concrete offered by IS (Indian Standards Codes) for all types of construction job which is depend upon performance, experience and testing. Concrete mixes have been selected according to IS 456-2000 and are available in a variety of grades, including M10, M15, M20, M25, M30, M35 and M40. The mix is represented by M in this instance, and numbers indicate the mix's 28-day cube strength in N/mm2.

Table 3.4 Different grades and their compressive strength

Grade of Concrete	Mix Ratio (cement : sand : aggregates)	Compressive Strength MPa (N/mm2)
M 5	1 : 5 : 10	5
M 7.5	1 : 4 : 8	7.5
M 10	1 : 3 : 6	10
M 15	1 : 2 : 4	15
M 20	1 : 1.5 : 3	20
M 25	1 : 1 : 2	25

M15 concrete is essential for providing the structural integrity required to support and endure lateral soil pressure while building retaining walls. Retaining walls are built to hold back soil and stop erosion; they are frequently used in road construction, landscaping, and other situations where it is necessary to control changes in ground elevation. Because of its modest compressive strength, M15 concrete is frequently used to build retaining walls in situations where the required load-bearing capacity is not too high.

The M15 concrete mix, which consists of one part cement, two parts sand, and four parts coarse aggregates, is ideal for building the retaining wall's body and foundation because it finds a compromise between strength and workability. The bonding power of the mix with reinforcing components, like steel bars or mesh, improves the structure's overall stability. When the main purpose of a retaining wall is to hold soil in conditions with low pressure, like those seen in gardens or landscaping projects, engineers choose for M15 concrete.

Calculation for materials requirement (Gravity Retaining Wall)

For casting M15 grade (1:2:4)

Volume of formwork = .06984 m^3

For dry concrete= 0.06984x1.54

= 0.10755m^3

Adding all ratio 1+2+4= 7

Calculating quantity of cement

(1/7) x .10755x1440

= 22.12 Kg (taking approx. 22 kg)

On the basis of ratio 1:2:4 sand and aggregate quantities are as follow:

Cement = 22 kg

Sand = 44 kg

Aggregate = 88 kg

As per IS 456 2000 clause 6.1.2 maximum free water cement ratio for M15 is .50

Water content = .50 x quantity of cement i.e. .50x22.12=11.06 litre.

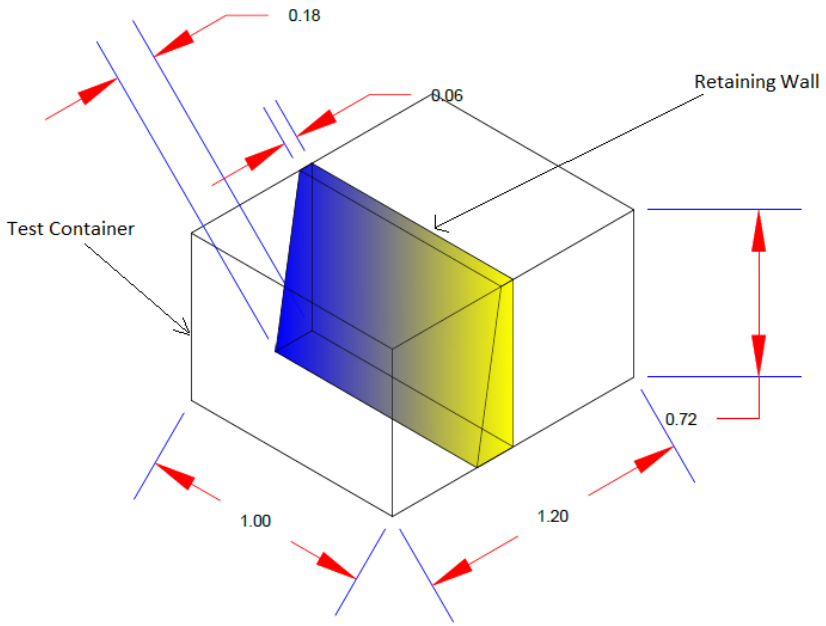

Fig.3.7 Test setup

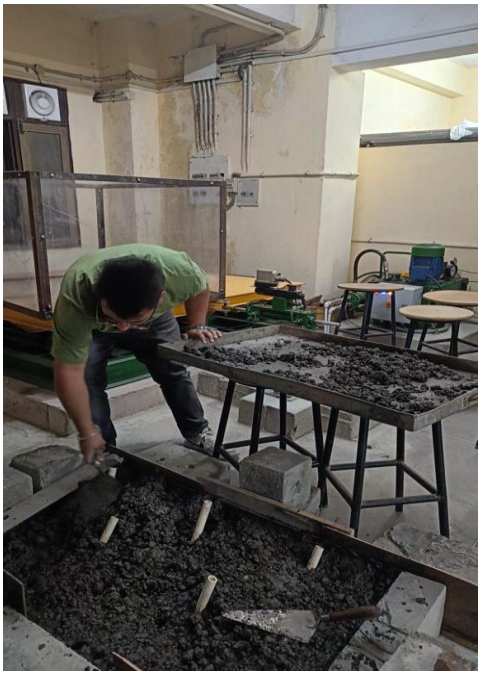

Fig.3.8 (a) Placing concrete in the formwork

Fig.3.8 (b) Casting of retaining wall

Fig.3.8 (c) Curing of retaining wall

Fig.3.8 (d) Curing with the help of cloth and sack

3.8 SHAKE TABLE TESTING

Shake table tests are a vital technique for investigating the performance of retaining walls under seismic conditions. These tests recreate earthquake scenarios to evaluate the stability and effectiveness of retaining walls, which are designed to hold back soil or other materials. By simulating real-world seismic events, engineers can observe the dynamic behavior of retaining walls, identify potential failure mechanisms, and improve design methods to enhance safety and durability.

3.8.1 Bhuj Earthquake

The Bhuj earthquake hit the Kutch district of Gujarat, India, on January 26, 2001. This catastrophic event had a moment magnitude of 7.7 and caused widespread destruction and significant loss of life.

Key Details

- Magnitude: 7.7 (Moment Magnitude Scale)
- Depth: Around 16 kilometers
- Epicenter: Near Bhuj town in the Kutch district of Gujarat

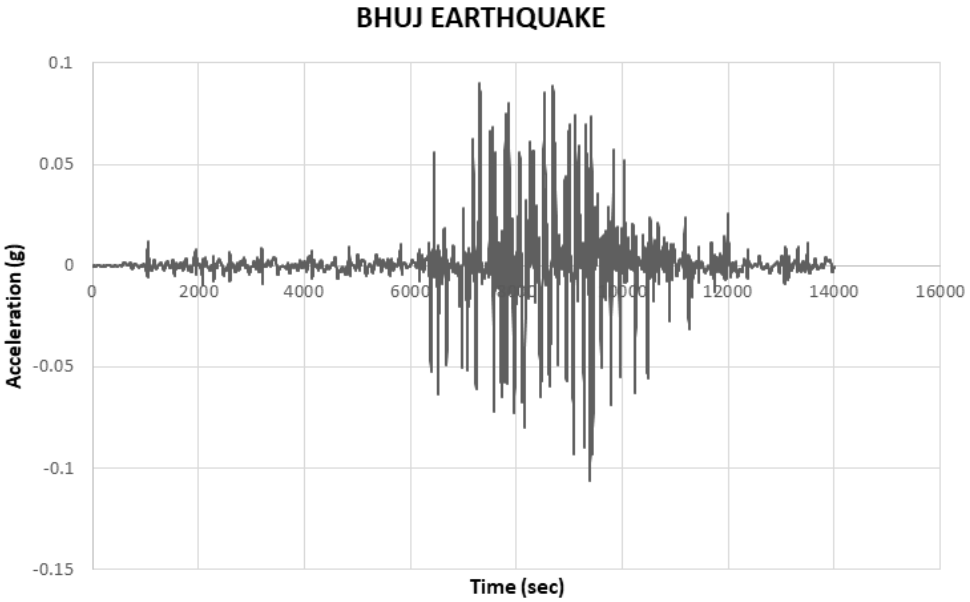

Fig.3.9 Bhuj Earthquake time history

3.8.2 Chile Earthquake

Chile has experienced many significant earthquakes due to its position along the Pacific Ring of Fire, a region in the Pacific Ocean basin known for frequent earthquakes and volcanic eruptions. One of the most notable earthquakes in Chilean history is the Great Chilean Earthquake, also called the Valdivia Earthquake.

Key Details

- Magnitude: 9.5 (Moment Magnitude Scale), the strongest earthquake ever recorded
- Epicenter: Near Valdivia in southern Chile
- Depth: Approximately 33 kilometers

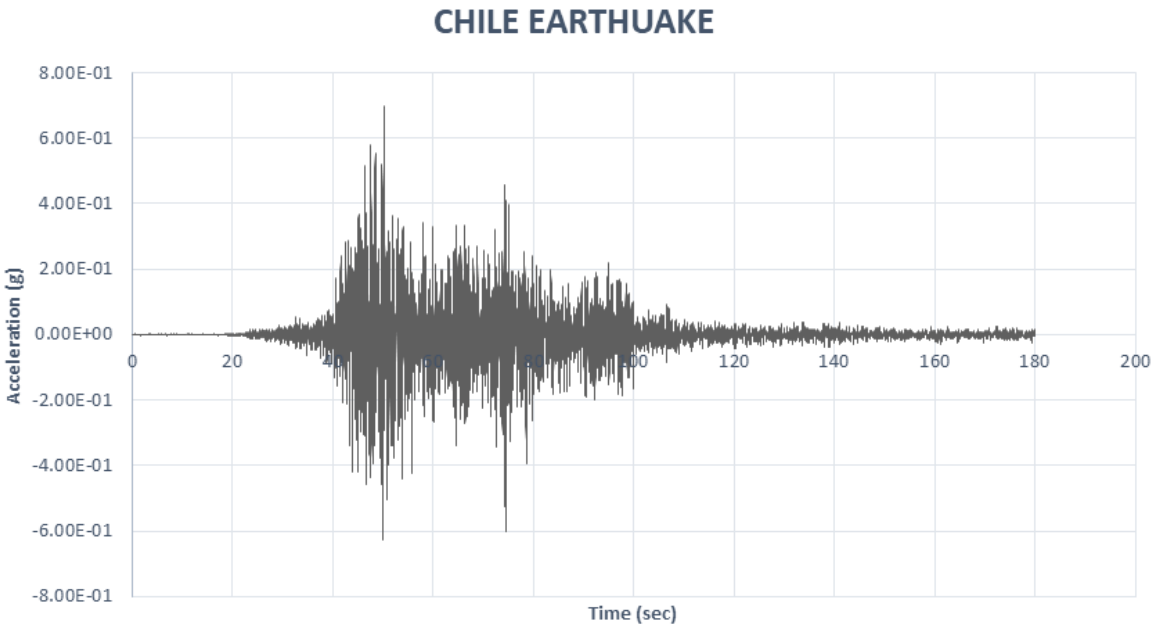

Fig. 3.10 Chile Earthquake time history

By replicating the ground motion characteristics of these significant earthquakes, we examined how retaining walls respond to intense shaking. The Bhuj earthquake, known for its high magnitude and devastating impact, serves as a case study for assessing the effects of prolonged ground motion and intense shaking. Similarly, the distinct seismic patterns of the Chile earthquake enable the evaluation of retaining walls under varied dynamic conditions. During these tests, retaining wall models are subjected to sine wave inputs that mimic the frequency and amplitude of the actual earthquake records. This approach helps identify potential vulnerabilities, such as sliding, tilting,

or overturning, and enhances our understanding of backfill soil behavior.

Retaining wall is tested under sinusoidal excitation. Sine wave with 1Hz frequency and amplitude increasing from 2 to 5 Vpp were given excitation. One accelerometer was placed in table and then on top of the wall in the whole experiment. Along with accelerometer, four strain gauges were used to check the strains coming in the wall and soil mass. Placement of accelerometer and strain gauges were shown in figure 3.12.

The configuration of the retaining wall and soil in the test container was carefully designed as shown in figure 3.11 to replicate real-world conditions. By positioning the retaining wall model inside the container, we filled the area behind it with backfill soil to simulate typical field settings. To gauge the influence of rainfall, we gradually added water to the backfill soil in increments of 5%, 10%, and 15%, guaranteeing uniform distribution. This setup facilitated the observation of the wall's response to seismic activity and varying moisture levels, offering comprehensive insights into potential vulnerabilities such as sliding, tilting, or overturning during simulated Bhuj and Chile earthquake scenarios.

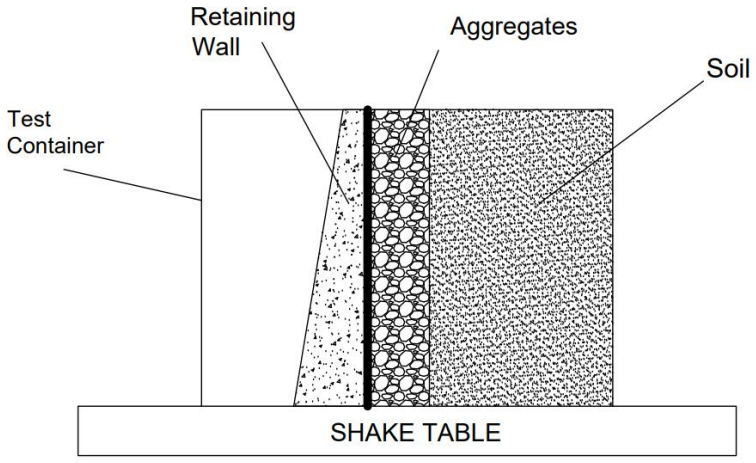

Fig. 3.11 Retaining wall with aggregate and soil

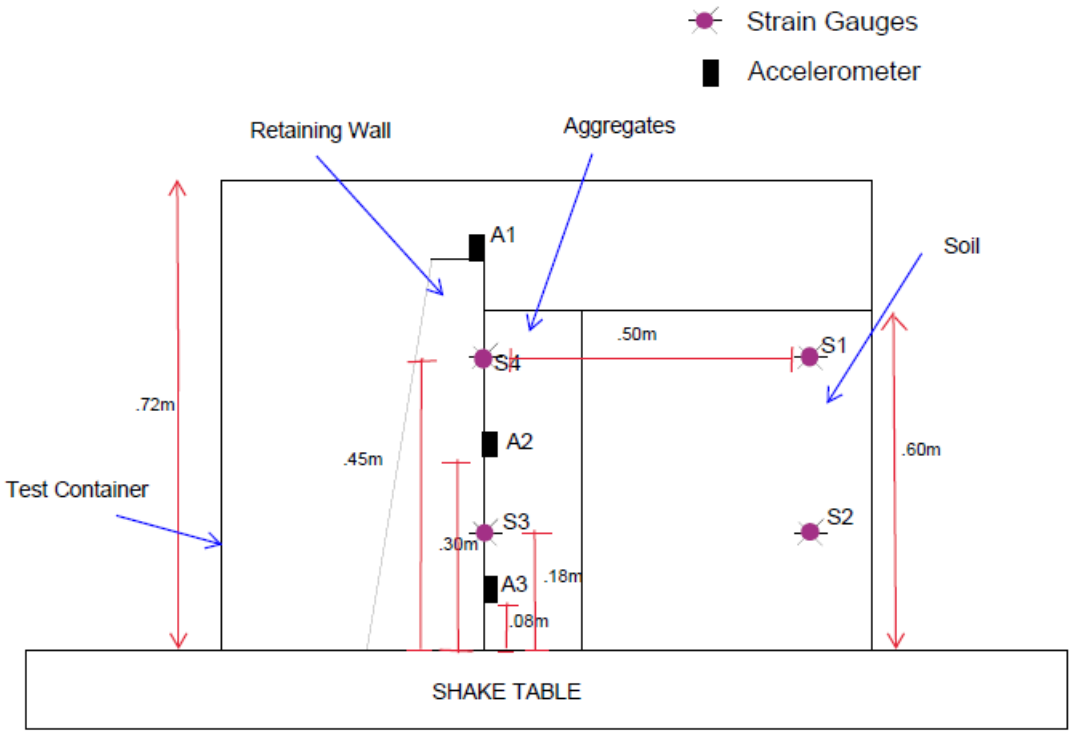

Fig. 3.12 Retaining wall and sensor arrangement

Table 3.5 Different Earthquake used with their frequency and PGA

Earthquake	Frequency	Peak Ground Acceleration			
Sine wave	1Hz	.05	.1g	.15g	.2g
Bhuj Earthquake	14.30mHz	.38g	.53g	.67g	.78g
Chile Earthquake	5.500mHz	.35g	.43g	.46g	.53g

Fig. 3.13 (a) Strain gauges placement

Fig. 3.13 (b) Placement of accelerometer

Fig. 3.14 (a) Shake table with whole setup

Fig. 3.14 (b) Retaining Wall with Backfill layers

Fig. 3.14 (c) Retaining Wall with Backfill

Fig. 3.15 Retaining Wall with Backfill failure

The shaking table tests included an essential phase where water was introduced to the backfill soil to simulate varying moisture conditions. Figure 3.16 shows the process of adding water to the soil at specific levels of 0%, 5%, 10%, and 15% by weight. This step was crucial for replicating real-world scenarios, particularly in regions such as Himachal Pradesh, which are prone to heavy rainfall and seismic events.

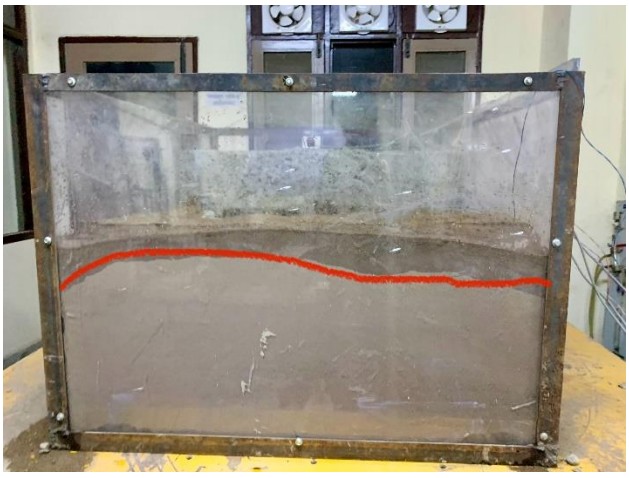

Fig. 3.16 (a) Retaining Wall with 5% water

Fig. 3.16 (b) Water flow path

Fig. 3.16 (c) Retaining Wall with 10% water

Fig. 3.16 (d) Retaining Wall with 15% water

CHAPTER 4

MODELLING AND ANALYSIS

4.1 GENERAL

Retaining walls play a vital role in holding back soil or other materials. Designing and analyzing these walls necessitates a thorough understanding of the interactions between the wall and the material it retains. Finite Element Analysis (FEA) software such as Abaqus is particularly effective for conducting detailed simulations to predict the behavior of retaining walls under various conditions. Accurate analysis of retaining walls is essential for ensuring their stability and safety, thereby preventing potential failures that could result in significant economic losses and safety risks. FEA tools like Abaqus enable engineers to model complex interactions and material behaviors, offering valuable insights into stress distribution, possible deformations, and failure mechanisms.

Modeling Different Types of Retaining Walls in Abaqus

Retaining walls come in various types, each with distinct structural characteristics and applications. Common types include gravity retaining walls, cantilever retaining walls, and reinforced soil retaining walls. Here's a guide on how to model these different types of retaining walls in Abaqus:

4.1.1 Geometry Creation

Utilize the part module in Abaqus CAE to construct the geometry for the retaining wall and the adjacent soil. The wall is generally represented as a solid block, featuring a wider base that narrows towards the top.

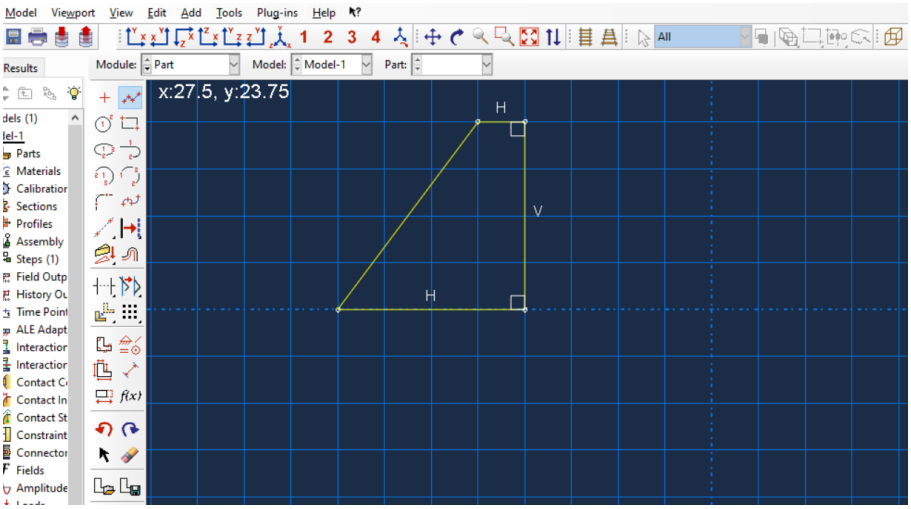

Fig. 4.1 Retaining geometry

4.1.2 Material Properties

Specify the material properties for the concrete wall, which include its density, Young's modulus, and Poisson's ratio.

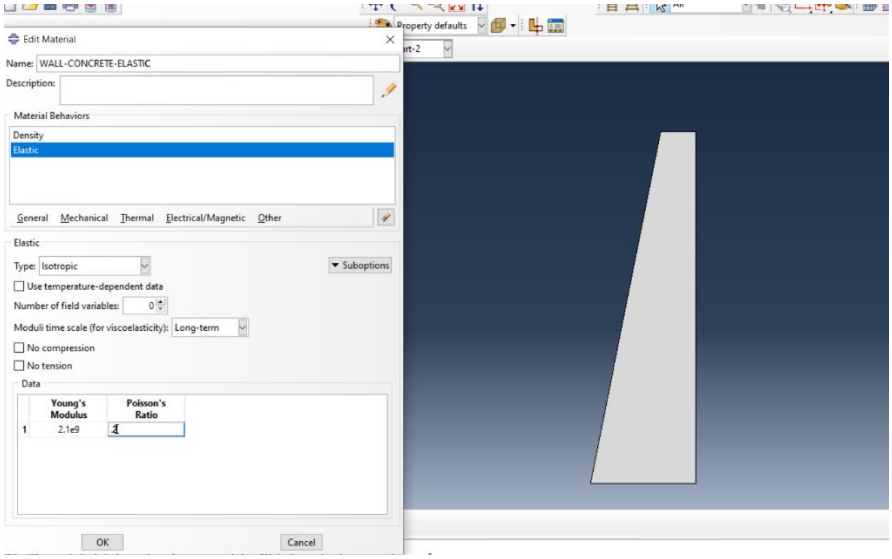

Fig. 4.2 Assigning Properties

4.1.3 Assembly and Interaction Properties

Establish the contact interaction between the wall and the soil, incorporating suitable friction properties to accurately represent their interface behavior.

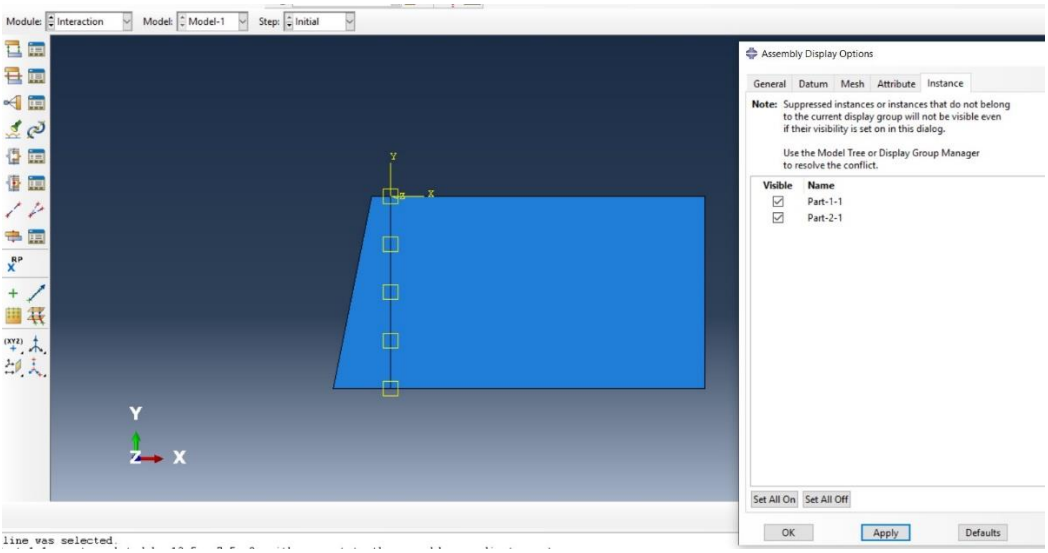

Fig. 4.3 Interaction of backfill and retaining wall

4.1.4 Analysis Steps

Configure the initial step for geostatic stress initialization. Next, create additional steps to model the construction sequences and the application of loads. If required, include nonlinear analysis steps to accurately represent the behavior of both the soil and the retaining wall.

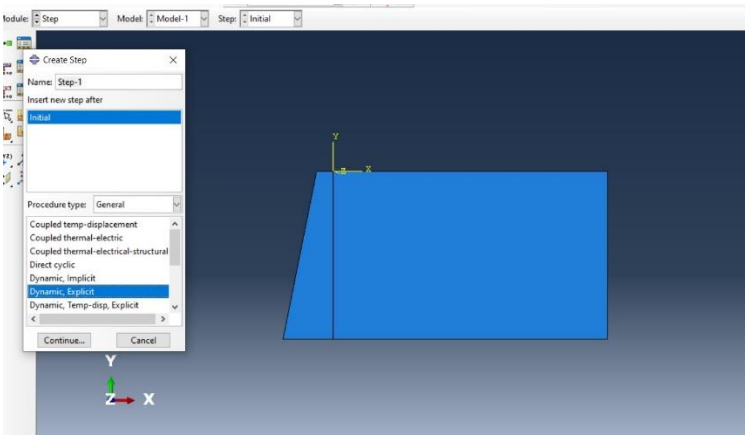

Fig. 4.4 Creating steps

4.1.5 Boundary Conditions and Loads

Securely anchor the bottom of both the wall and soil to replicate a rigid base. Following this, administer gravity loads to both the wall and soil. Moreover, introduce lateral earth pressure on the rear face of the wall.

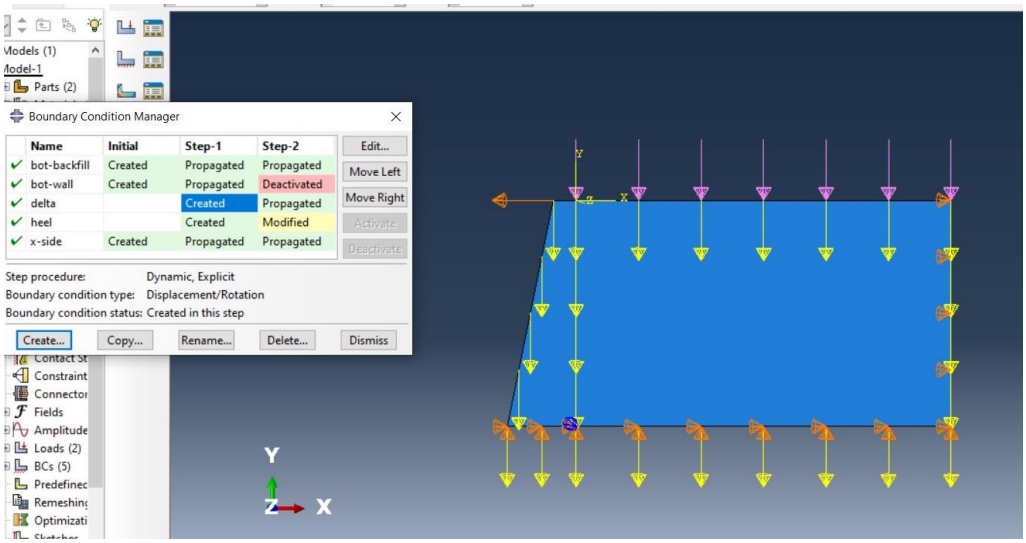

Fig. 4.5 Assigning Loads and Boundary condition

4.1.6 Meshing

Create a mesh for the geometry using suitable element types. Abaqus education license doesn't allow to mesh the model more precisely as its only limited to 1000 nodes.

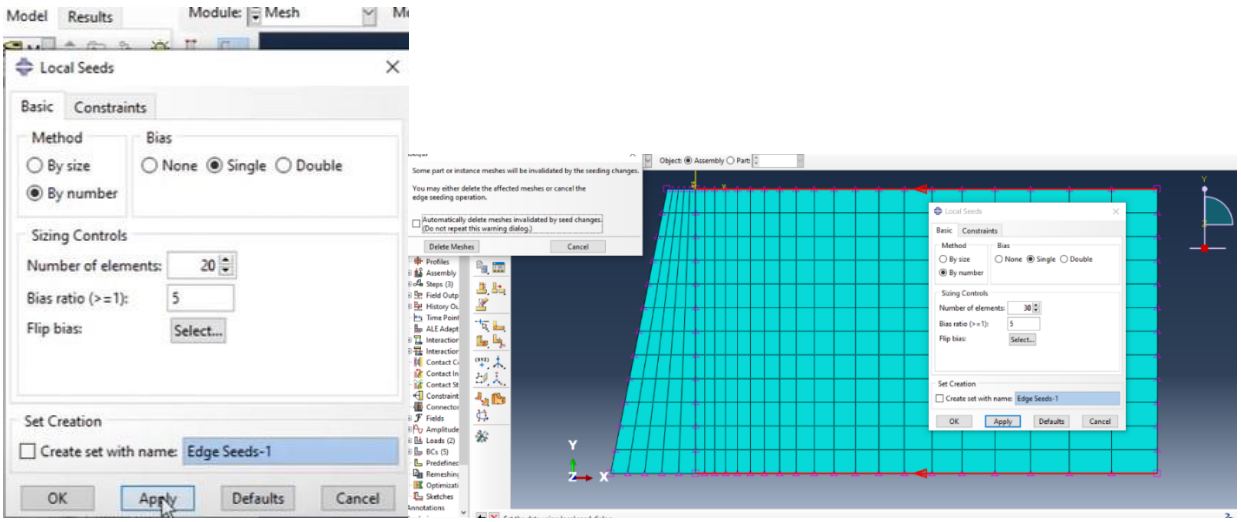

Fig. 4.6 Meshing

4.1.7 Running the Analysis

Submit the analysis job in Abaqus/Standard or Abaqus/Explicit, selecting the appropriate solver based on the complexity and nature of the problem.

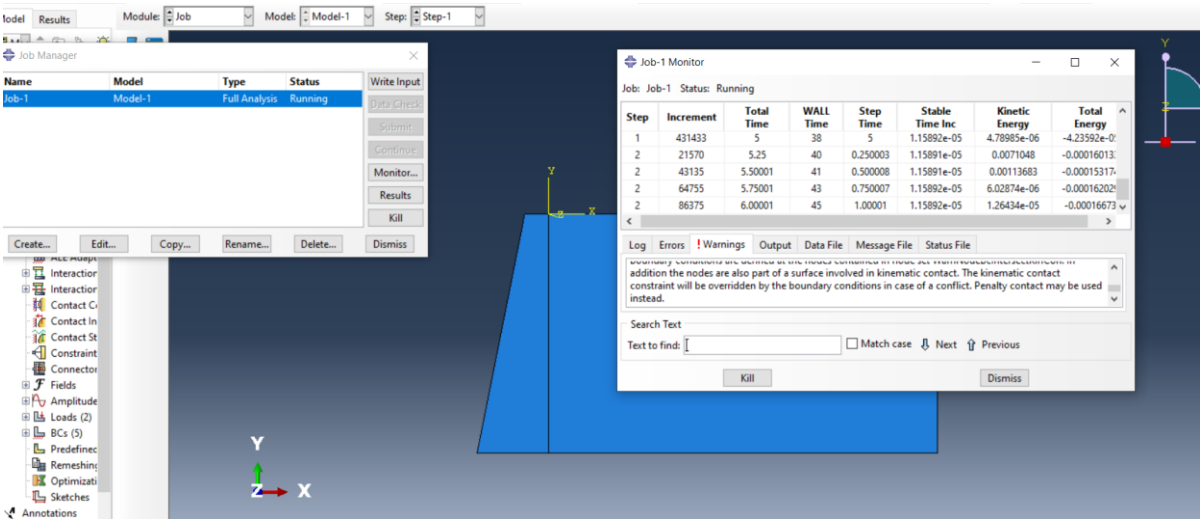

Fig. 4.7 Analysis of model

4.1.8 Creating Job and Monitoring

Analyze the results to observe displacement, stress distribution, and potential failure mechanisms. Utilize contour plots, deformation plots, and other visualization tools available in Abaqus/CAE to interpret and understand the outcomes.

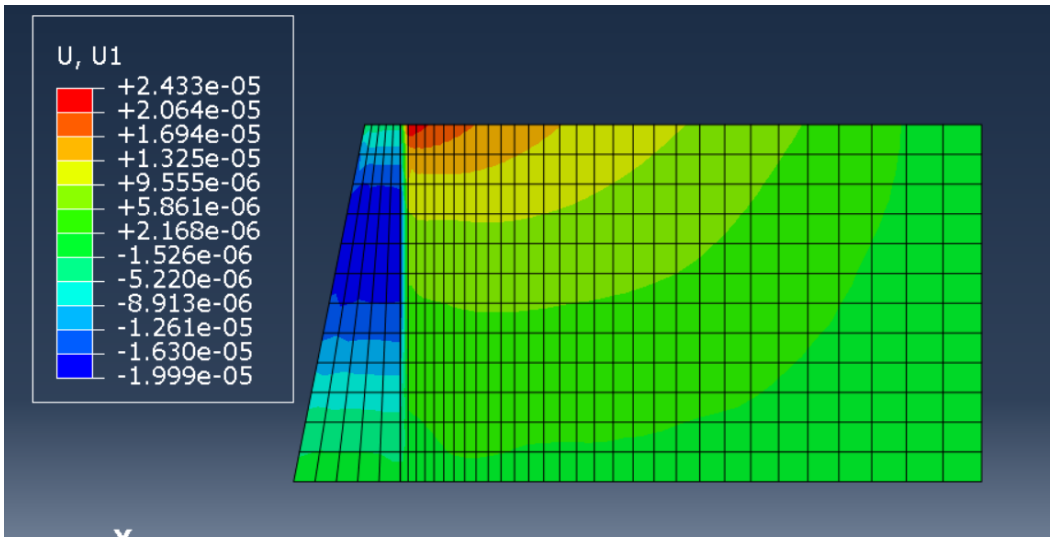

Fig. 4.8 Displacements result

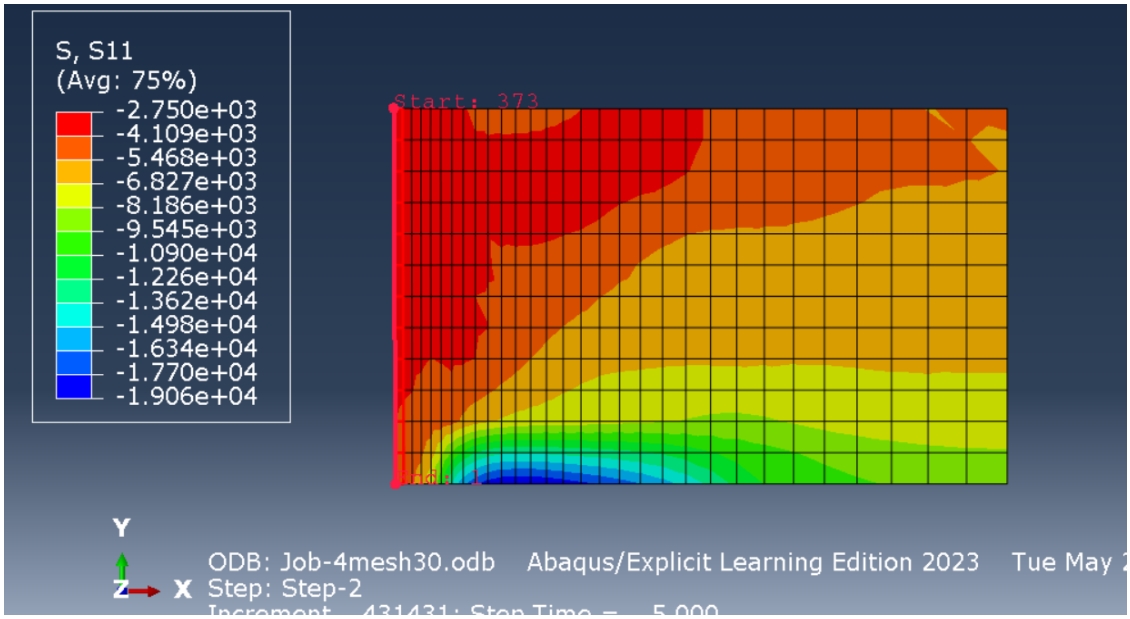

Fig. 4.7 Stress results

Following these steps enables engineers to proficiently model and analyze various types of retaining walls in Abaqus, guaranteeing they adhere to safety and performance standards under diverse loading conditions.

CHAPTER 5

RESULT

5.1 SHAKE TABLE RESULTS

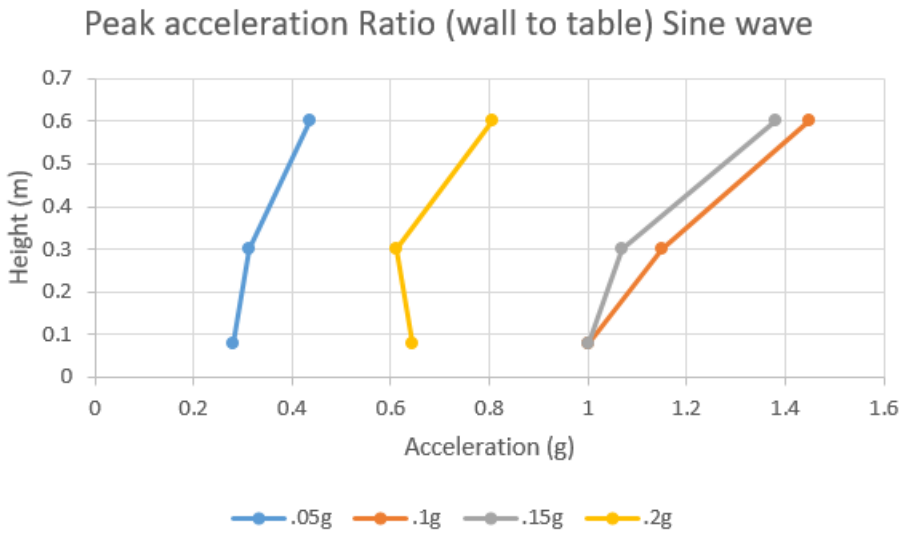

Fig. 5.1 Peak acceleration ratio (wall to table) of Sine wave

The graph titled "Peak acceleration Ratio (wall to table) Sine wave" depicts the relationship between acceleration (measured in g) and height (measured in meters) for different peak accelerations of a sine wave. There are four different datasets represented in the graph, each corresponding to a specific peak acceleration value: 0.05g, 0.1g, 0.15g, and 0.2g.

0.05g shows a steep increase in height with increasing acceleration, starting from around 0.2g and ending just below 0.5g. 0.1g begins at an acceleration slightly above 1g and shows a moderate increase in height as acceleration increases, ending just above 1.4g.0.15g starts from an acceleration around 1g and shows a slight increase in height, reaching approximately 1.4g. 0.2g starts around 0.6g and shows a dramatic increase in height, ending slightly below 0.9g.

Each dataset reveals how height varies with acceleration for a given peak acceleration value of a sine wave. The patterns indicate that as the peak acceleration increases, the height at which these values occur also increases. The data points illustrate a non-linear relationship between height and acceleration for different peak accelerations.

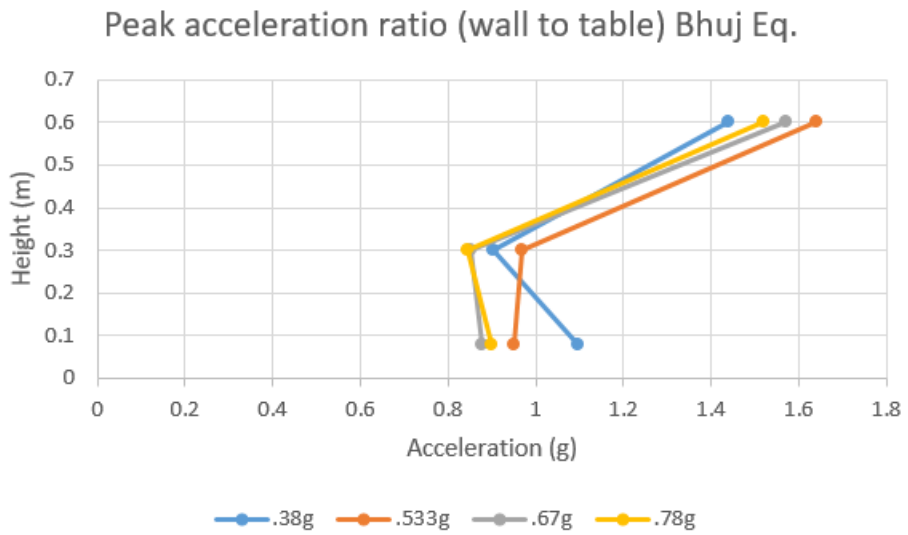

Fig. 5.2 Peak acceleration ratio (wall to table) of Bhuj Eq.

0.38g starts just below 1g of acceleration and increases in height sharply, reaching above 1.6g with a height just under 0.7 meters. 0.533g starts slightly above 0.8g and shows an initial dip in height before rising steadily, ending above 1.6g with a height of around 0.6 meters. 0.67g starts around 0.8g of acceleration and initially decreases in height before increasing steadily, peaking above 1.4g with a height close to 0.6 meters. 0.78g begins just below 0.8g and follows a similar pattern of an initial decrease in height before rising sharply, ending around 1.4g with a height close to 0.6 meters.

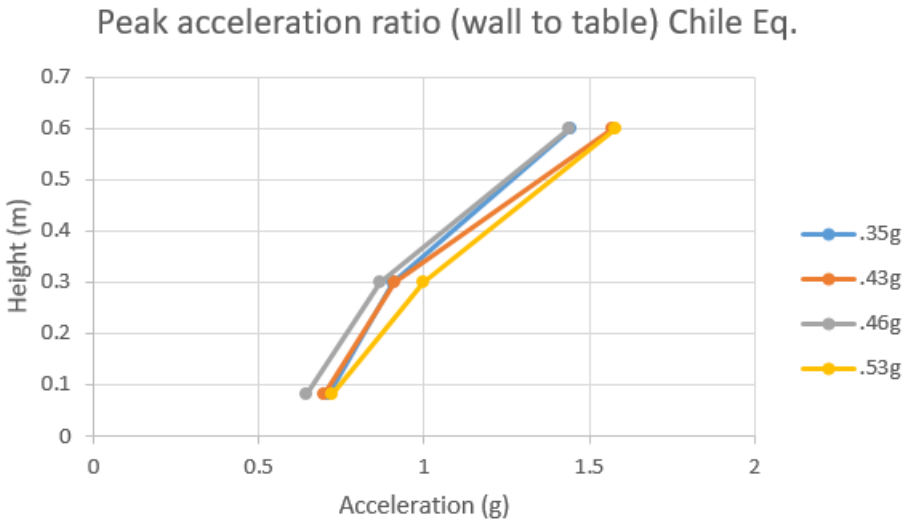

Fig. 5.3 Peak acceleration ratio (wall to table) of Chile Eq.

The graph titled "Acceleration with different water % (Bhuj Eq.)" shows the relationship between acceleration (measured in g) and height (measured in meters) for different percentages of water content during the Bhuj earthquake. There are four datasets represented in the graph, each corresponding to a specific water content: 0%, 5%, 10%, and 15%.

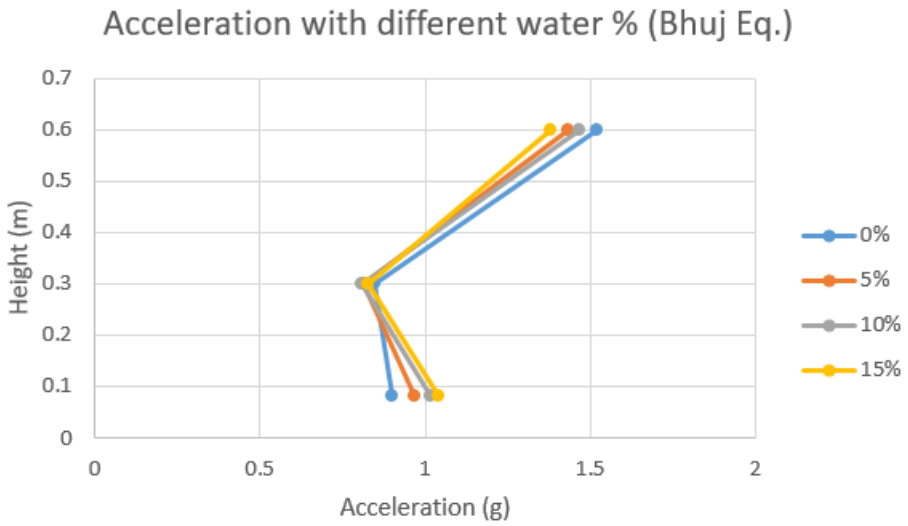

Fig. 5.4 Peak acceleration wrt water content (Bhuj Eq.)

0% water starts at an acceleration slightly above 0.5g and initially dips in height before increasing sharply, reaching a height of around 0.6 meters at approximately 1.5g acceleration. 5% water begins at an acceleration just below 1g and follows a similar pattern of an initial decrease in height, then rising steadily to reach a height slightly below 0.6 meters at around 1.5g acceleration. 10% water starts just below 1g of acceleration with an initial dip in height, followed by a steady increase, peaking at a height just below 0.6 meters around 1.5g acceleration. 15% water begins at an acceleration just below 1g, showing an initial drop in height before a sharp increase, reaching a height close to 0.6 meters at around 1.5g acceleration.

Each dataset illustrates how the height varies with acceleration for different water contents during the Bhuj earthquake. The trends indicate that higher water content doesn't significantly alter the general pattern of an initial dip followed by a sharp rise in height as acceleration increases. The final heights achieved at around 1.5g acceleration are relatively consistent across all water content levels, suggesting that the presence of water influences the initial response but converges at higher accelerations.

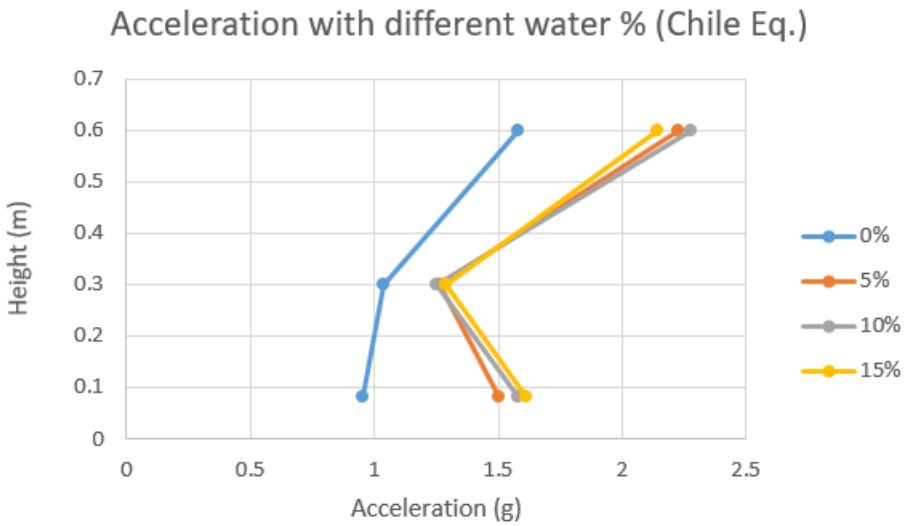

Fig. 5.5 Peak acceleration wrt water content (Chile Eq.)

The graph shows the relationship between acceleration (in g) and height (in meters) for different percentages of water content (0%, 5%, 10%, and 15%) during the Chile earthquake scenario.

0% water initially increases sharply in height with a small increase in acceleration, peaking at about 0.6 meters height at 1.5g, then decreases to around 0.3 meters height with further acceleration. 5% water starts at a low height, increases steadily to around 0.2 meters at 1.5g, and then decreases slightly. 10% water shows a slight increase in height to around 0.1 meters at 1.5g, then slightly decreases. 15% water similar to the 10% water curve, shows a slight initial increase to around 0.1 meters at 1.5g, and then a slight decrease.

Overall, the 0% water content shows a more pronounced change in height with varying acceleration compared to other water contents, which show more modest changes.

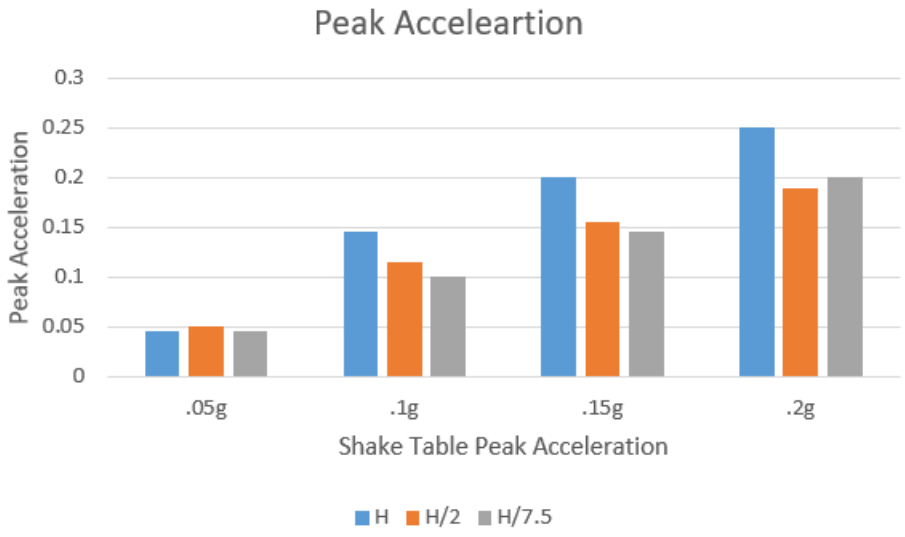

Fig. 5.6 Peak acceleration wrt Shake table peak acceleration (sine wave)

Displays peak acceleration for shake table peak accelerations of 0.05g, 0.1g, 0.15g, and 0.2g. H/2 (blue bars) generally shows higher peak accelerations compared to H/7.5 (gray bars).The peak acceleration increases as the shake table peak acceleration increases for both heights.

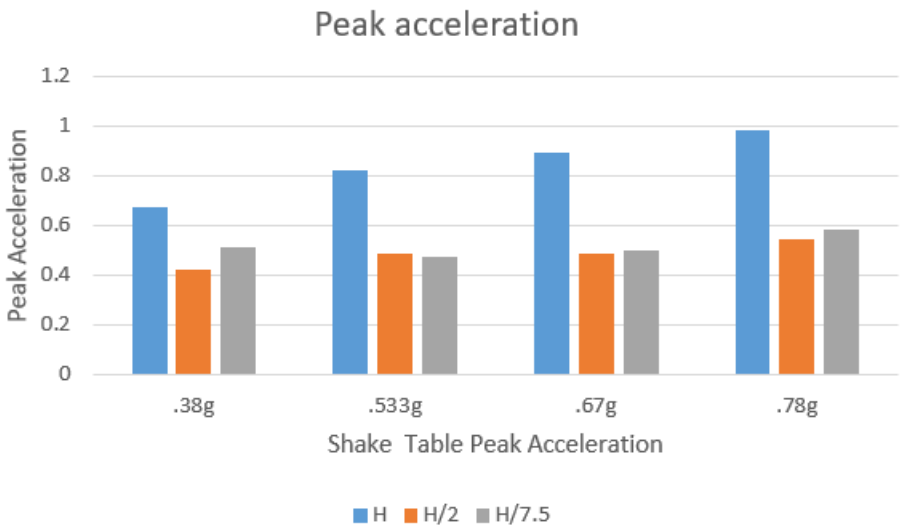

Fig. 5.7 Peak acceleration wrt Shake table peak acceleration (Bhuj Eq.)

Illustrates peak acceleration for shake table peak accelerations of 0.38g, 0.533g, 0.67g, and 0.78g. The trend of higher peak accelerations for H/2 compared to H/7.5 persists. Peak acceleration consistently rises with increased shake table acceleration.

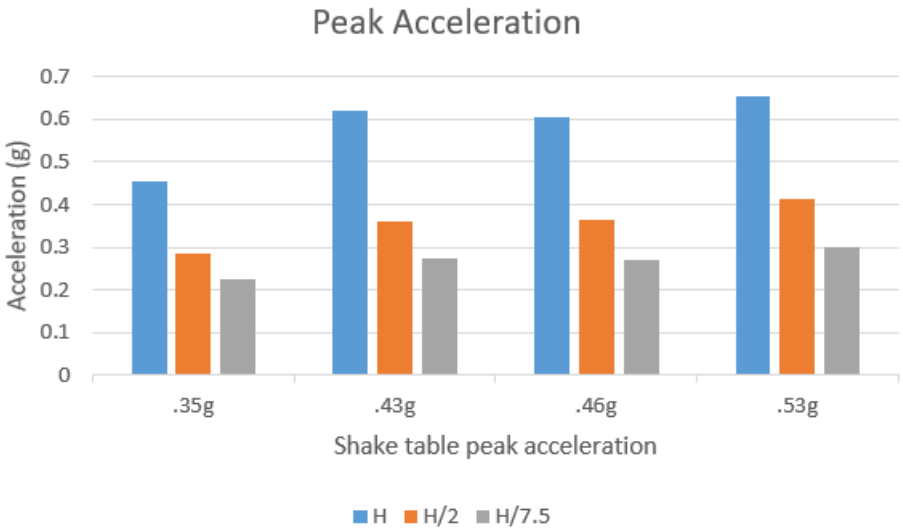

Fig. 5.8 Peak acceleration wrt Shake table peak acceleration (Chile Eq.)

Shows peak acceleration for shake table peak accelerations of 0.35g, 0.43g, 0.46g, and 0.53g.

H/2 again exhibits higher peak accelerations than H/7.5. A noticeable increase in peak acceleration with increasing shake table peak acceleration for both heights is observed.

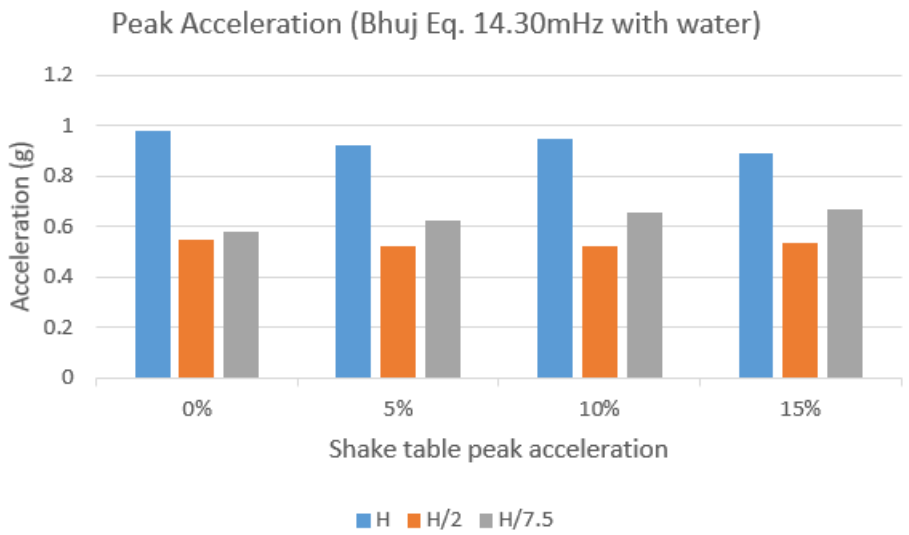

Fig. 5.9 Peak acceleration wrt Shake table peak acceleration with Water (Bhuj Eq.)

Analyzes the impact of water content (0%, 5%, 10%, and 15%) on peak acceleration. For each water content level, H/2 shows higher peak accelerations than H/7.5. The presence of water affects peak accelerations, but H/2 maintains a higher value across all water content percentages.

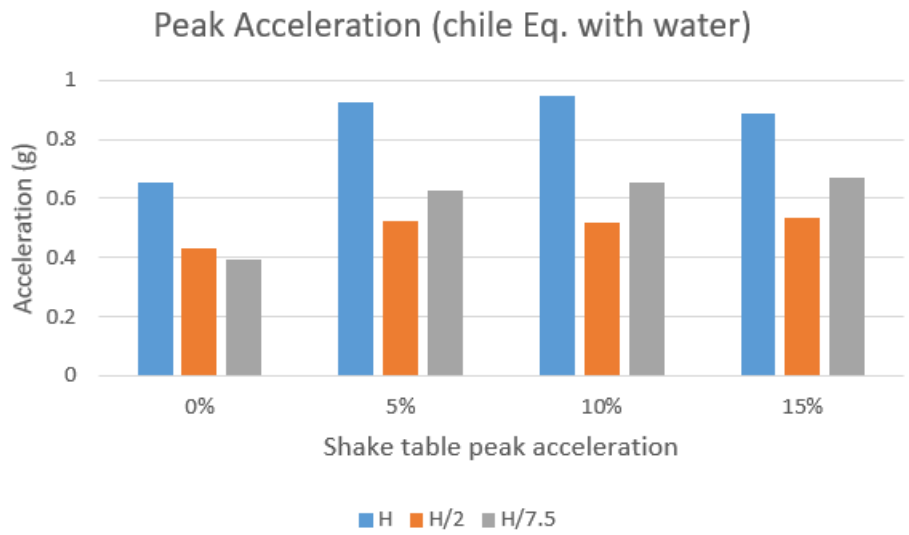

Fig. 5.10 Peak acceleration wrt Shake table peak acceleration with Water (Chile Eq.)

Table 5.1 Peak Strains when subjected to Bhuj Eq.

Water Content	S1	S2	S3	S4
0%	0.0000006	0.0000012	0.0000032	0.0000026
5%	6.2E-07	0.0000014	0.0000039	0.0000027
10%	0.0000008	0.0000016	0.0000043	0.0000031
15%	0.0000012	0.000002	0.0000048	0.0000034

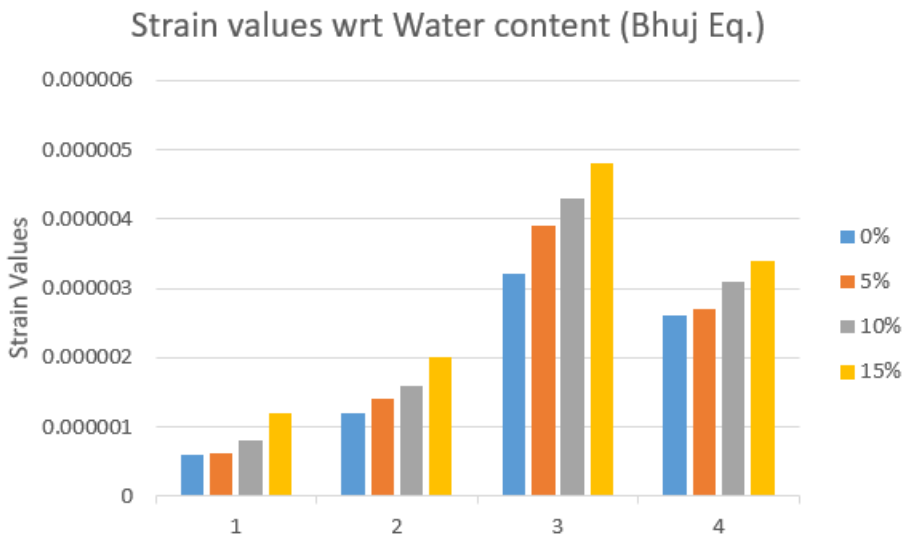

Fig. 5.11 Strain values wrt water content (Bhuj Eq.)

The graph illustrates the strain values associated with varying water content percentages (0%, 5%, 10%, and 15%) during the Bhuj earthquake simulation, plotted across four different scenarios or measurements (labeled 1, 2, 3, and 4). In Scenario 1, strain values are relatively low and similar across all water content levels, with a slight increase noted for the 15% water content. Moving to Scenario 2, strain values show a slight increase compared to Scenario 1, with the highest value again seen at 15% water content. In Scenario 3, there is a more noticeable rise in strain values, with the highest strain observed for 15% water content, followed sequentially by 10%, 5%, and 0%. Finally, in Scenario 4, strain values remain elevated, with 15% water content consistently showing the highest strain, followed by 10%, 0%, and 5%. Overall, the strain values increase progressively from Scenario 1 to Scenario 4, and higher water content, particularly at 15%, generally results in higher strain values across all scenarios.

Table 5.2 Peak Strains when subjected to Chile Eq.

Water Content	S1	S2	S3	S4
0%	0.0000004	0.0000012	0.0000031	0.0000026
5%	0.0000006	1.39E-06	3.85E-06	0.0000034
10%	0.0000008	1.48E-06	0.0000047	3.58E-06
15%	0.0000012	0.0000021	0.000005	4.25E-06

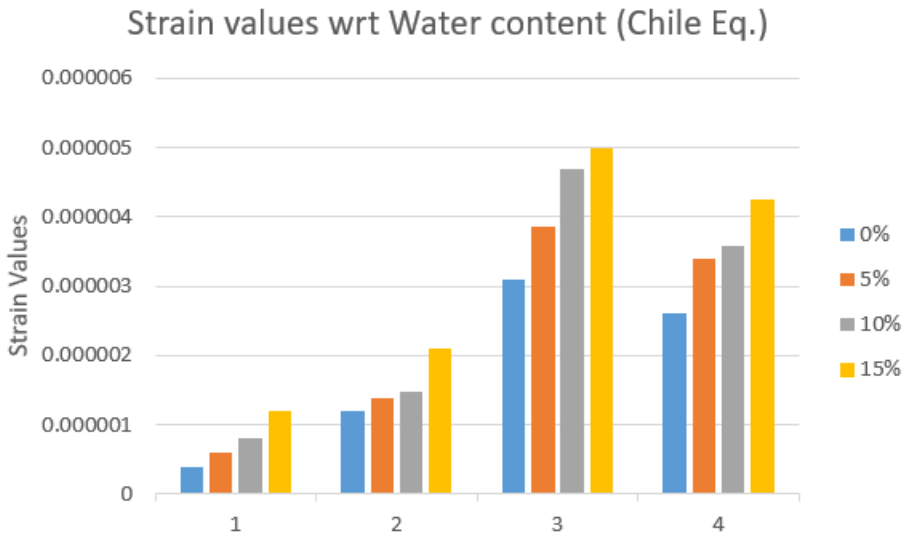

Fig. 5.12 Strain values wrt water content (Chile Eq.)

The bar chart titled "Strain values wrt Water content (Chile Eq.)" illustrates the strain values of a material under different water content conditions (0%, 5%, 10%, and 15%) across four different samples. The x-axis represents the sample numbers (1 through 4), while the y-axis represents the strain values.

From the chart, it is evident that the strain values increase with higher water content for all samples. Sample 1 shows a minimal increase in strain values, whereas samples 3 and 4 exhibit a significant rise, particularly at 10% and 15% water content. Sample 3 has the highest strain value at 15% water content, reaching approximately 0.000005. Overall, the data suggests a direct correlation between increased water content and higher strain values across all samples, with the most pronounced effects seen in samples 3 and 4.

5.2 Abaqus Results

Figure 5.13 shows the displacement field of the retaining wall. The color gradient ranges from dark blue, indicating the least displacement (-6.957e-05), to dark red, showing the maximum displacement (+3.139e-05). The displacement is primarily concentrated at the base and lower sections of the wall, with minimal displacement observed at the top and right side. This suggests that the lower part of the retaining wall experiences significant movement, likely due to pressure or load exerted from the soil or other forces behind the wall.

Figure 5.14 presents the stress distribution within the retaining wall, indicated by the S11 stress component. The stress ranges from -1.906e+04 (blue, indicating compression) to +2.750e+03 (red, indicating tension). High compressive stresses are observed at the base and lower left corner of the wall, while tensile stresses are distributed more towards the upper regions. The stress concentration patterns reflect the structural response of the wall under load, with compressive forces dominating the regions close to the load application point and tensile forces spreading out towards the free edges.

Overall, these visualizations highlight the areas of critical displacement and stress within the retaining wall, crucial for assessing the wall's structural integrity and performance under load conditions.

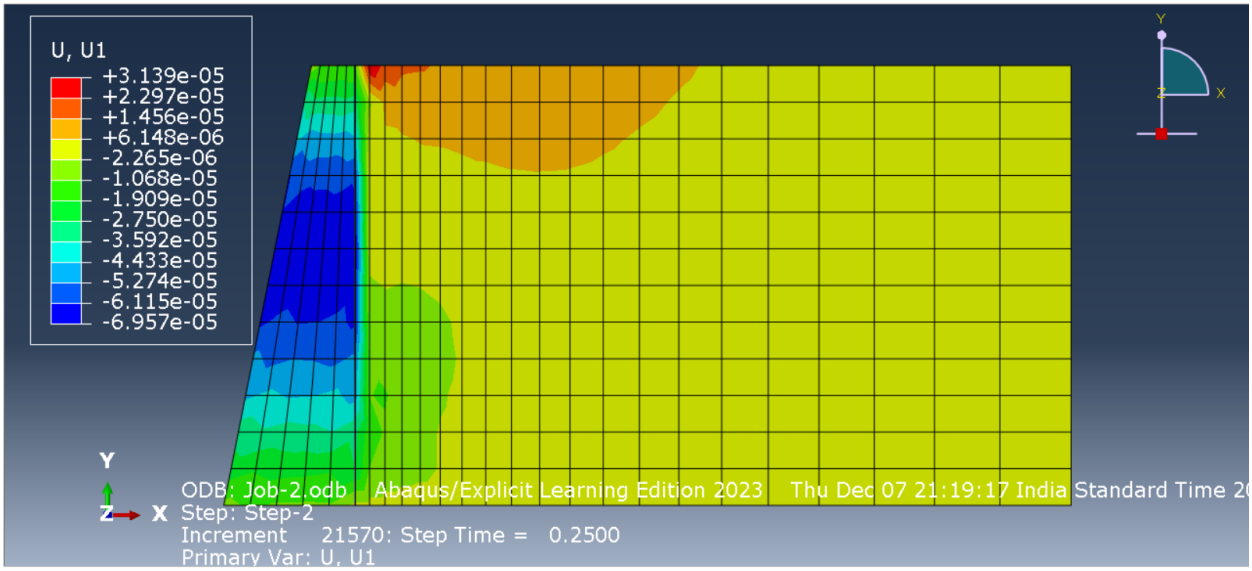

Fig. 5.13 Displacement Visualization

Figure 5.14 shows the distribution of the S11 stress component in the retaining wall. The stress ranges from -1.906e+04 (high compressive stress, blue) to +2.750e+03 (tensile stress, red). The stress distribution indicates that compressive stresses are more prominent at the base and lower left corner, while tensile stresses are found in the upper regions.

Figure 5.15 illustrates the von Mises stress distribution in the retaining wall. The stress ranges from 9.286e+02 to +7.062e+04, with higher stress concentrations observed near the base and the left side, indicating critical areas that may need reinforcement to prevent structural failure.

Figure 5.16 Stress with Height (Top to Bottom) plots the S11 stress component along the height of the retaining wall from top to bottom. The graph shows variations in stress along the height, with peaks and troughs indicating areas of higher and lower stress, respectively. This detailed profile helps in understanding how the stress is distributed vertically in the wall.

Figure 5.17 presents the displacement (U1 component) along the height of the retaining wall. The displacement varies significantly, with the largest displacements occurring towards the bottom and a notable peak at the top, indicating where the wall experiences the most movement under load.

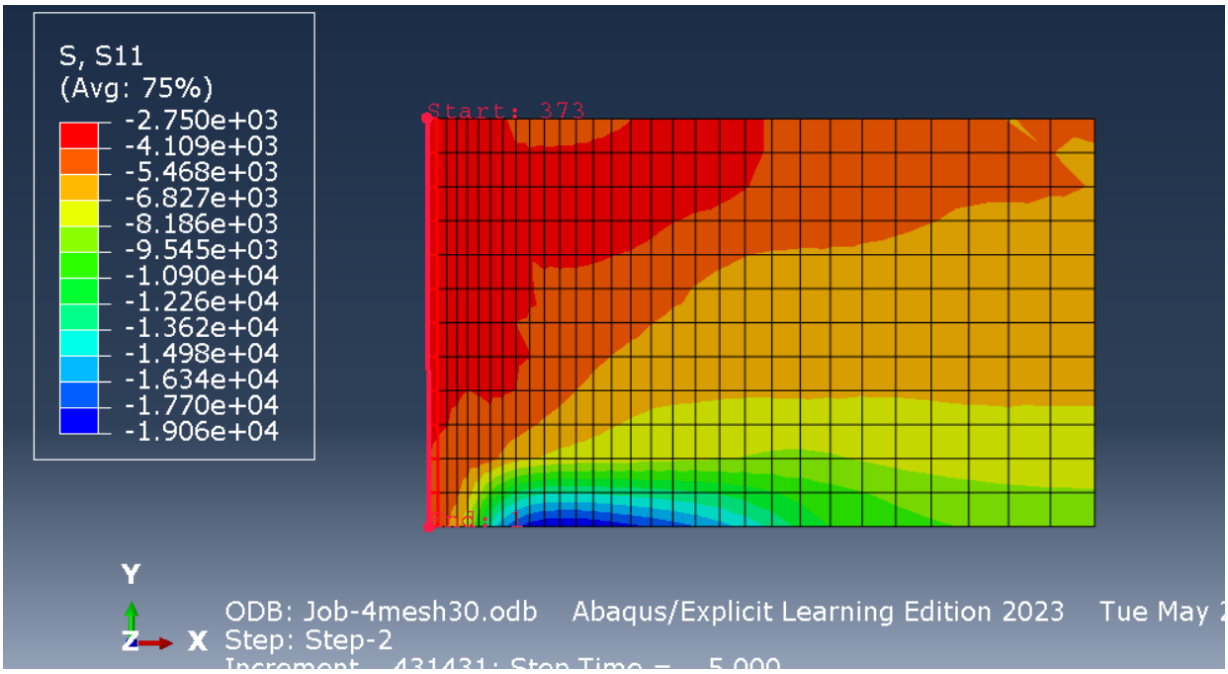

Fig. 5.14 Stress Visualization

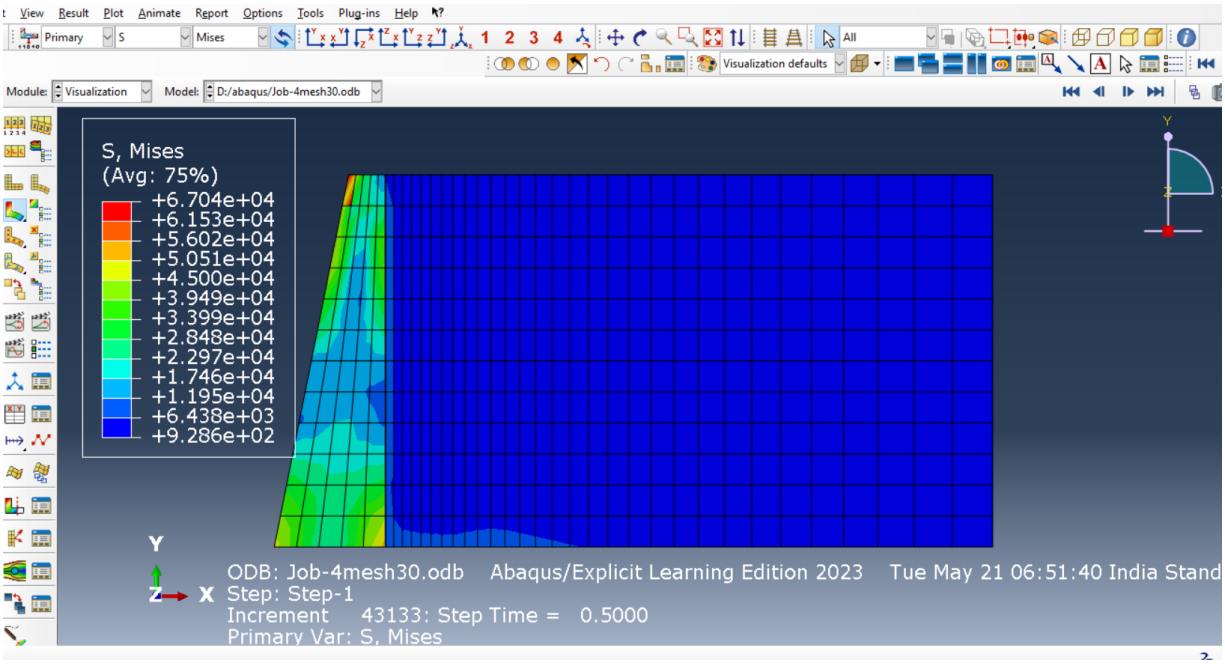

Fig. 5.15 Retaining wall Stress Visualization

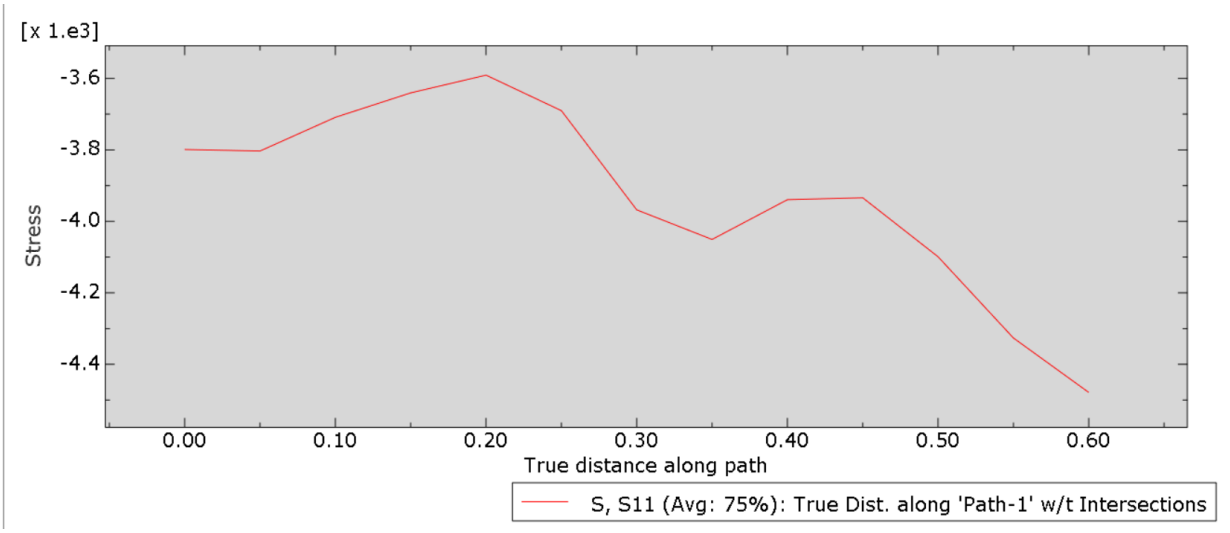

Fig. 5.16 Stress with height top to bottom

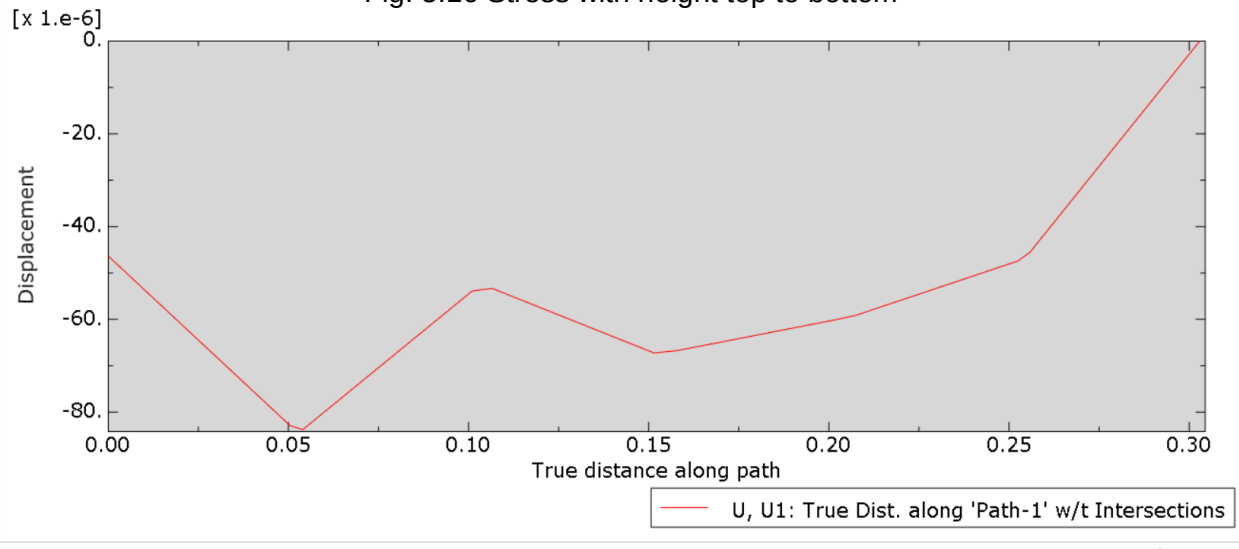

Fig. 5.17 Displacement with height top to bottom

These figures collectively provide a comprehensive overview of the structural behavior of the retaining wall under load, highlighting critical areas of stress and displacement. This analysis is crucial for designing effective reinforcement strategies to ensure the wall's stability and integrity.

Chapter 6
CONCLUSION

The study revealed that the seismic behavior of retaining walls is significantly influenced by the type of seismic excitation applied, with different seismic inputs, including sine wave inputs and historical earthquake records, resulting in varying responses in terms of wall stability and deformation. The investigation into the effect of different water content levels in the backfill soil on the wall's dynamic response showed that higher moisture content levels, such as 10% and 15%, led to increased instability and deformation compared to lower moisture levels, highlighting the importance of considering water content in retaining wall design and analysis. By combining physical shaking table tests with numerical simulations using ABAQUS, the study successfully provided a detailed understanding of stress distribution, failure mechanisms, and overall behavior of retaining walls under seismic loading, enhancing the accuracy of predictions and analysis. These findings have significant implications for the design and construction of retaining structures in earthquake-prone areas, as understanding the dynamic response of retaining walls under combined rainfall and seismic effects can help in developing more resilient infrastructure and improving safety measures.

REFERENCES

1. Matsuo, O., K. Yokoyama, and Y. Saito. "Shaking table tests and analyses of geosynthetic-reinforced soil retaining walls." *Geosynthetics International* 5.1-2 (1998): 97-126.
2. Ling, Hoe I., et al. "Large-scale shaking table tests on modular-block reinforced soil retaining walls." *Journal of Geotechnical and Geoenvironmental Engineering* 131.4 (2005): 465-476.
3. Ling, Hoe I., et al. "Seismic response of geocell retaining walls: experimental studies." *Journal of Geotechnical and Geoenvironmental Engineering* 135.4 (2009): 515-524.
4. Ma, Tsun Ming Quincy, et al. "Experimental evaluation of inter-storey drifts during the Cook Strait earthquake sequence." *New Zealand Society for Earthquake Engineering Technical Conference and AGM*. 2014.
5. Hidayati, Anissa Maria, R. W. Sri Prabandiyani, and I. Wayan Redana. "Laboratory Tests on Failure of Retaining Walls Caused by Sinusoidal Load." *Applied Mechanics and Materials* 776 (2015): 41-46.
6. Saleem, M. Umair, et al. "Shake table tests on FRP retrofitted masonry building models." *Journal of Composites for Construction* 20.5 (2016): 04016031.
7. Madhavi Latha, G., and G. S. Manju. "Seismic response of geocell retaining walls through shaking table tests." *International Journal of Geosynthetics and Ground Engineering* 2 (2016): 1-15.
8. Ai, Jie, Jinsong Gui, and Ding Chen. "The Analysis of Earth Pressure on Retaining Wall Based on Abaqus." *2016 5th International Conference on Sustainable Energy and Environment Engineering (ICSEEE 2016)*. Atlantis Press, 2016.
9. Johari, Ali, A. A. Javadi, and H. Najafi. "A genetic-based model to predict maximum lateral displacement of retaining wall in granular soil." *Scientia Iranica* 23.1 (2016): 54-65.
10. Li, Weiwei, et al. "In-plane strengthening effect of prefabricated concrete walls on masonry structures: Shaking table test." *Shock and Vibration* 2017 (2017).
11. Yazdandoust, Majid. "Investigation on the seismic performance of steel-strip reinforced-soil retaining walls using shaking table test." *Soil Dynamics and Earthquake Engineering* 97 (2017): 216-232.
12. Xu, Shi-Yu, KK Pabodha M. Kannangara, and Ertugrul Taciroglu. "Analysis of the stress distribution across a retaining wall backfill." *Computers and Geotechnics* 103 (2018): 13-25.
13. Lin, Yu-liang, Xue-ming Cheng, and Guo-lin Yang. "Shaking table test and numerical simulation on a combined retaining structure response to earthquake loading." *Soil Dynamics and Earthquake*

Engineering 108 (2018): 29-45.

14. Reyes, Juan C., et al. "Out-of-plane shaking table tests of full-scale historic adobe corner walls retrofitted with timber elements." *Earthquake Engineering & Structural Dynamics* 48.8 (2019): 888-909.
15. Ren, Feifan, Qiangqiang Huang, and Guan Wang. "Shaking table tests on reinforced soil retaining walls subjected to the combined effects of rainfall and earthquakes." *Engineering Geology 267* (2020): 105475.
16. Savalle, N., et al. "Dynamic behaviour of drystone retaining walls: shaking table scaled-down tests." *European Journal of Environmental and Civil Engineering* 26.10 (2020): 4527-4547
17. Ren, Feifan, Qiangqiang Huang, and Guan Wang. "Shaking table tests on reinforced soil retaining walls subjected to the combined effects of rainfall and earthquakes." *Engineering Geology* 267 (2020): 105475.
18. Tiwari, Rohit, and Nelson Lam. "Modelling of seismic actions in earth retaining walls and comparison with shaker table experiment." *Soil Dynamics and Earthquake Engineering* 150 (2021): 106939.
19. Ma, Shuzhi, Hongbiao Jia, and Xiaolang Liu. "Effect of the Wall-Back Inclination Angle on the Inertial Loading Distribution along Gravity-Retaining Walls: An Experimental Study on the Shaking Table Test." *Advances in Civil Engineering* 2022 (2022).
20. Sundaravel, V., and G. R. Dodagoudar. "Finite Element Analysis of Reinforced Earth Retaining Structures: Material Models and Performance Assessment." *Indian Geotechnical Journal* (2024): 1-20.